

Review

Not peer-reviewed version

Hydroxyapatite as a Material for Transplantology: Clinical Experience and Prospects of Application

Vitaliy Markelov , [Kseniya Danilko](#) ^{*} , Vadim Solntzev , [Svetlana Piatnitskaia](#) , Olga Shangina , [Azat Bilyalov](#) , Svyatoslav Chugunov , Iskander Akhatov

Posted Date: 28 November 2023

doi: 10.20944/preprints202311.1701.v1

Keywords: hydroxyapatite; bone grafting; nanoparticles; immune response; mitochondria



Preprints.org is a free multidiscipline platform providing preprint service that is dedicated to making early versions of research outputs permanently available and citable. Preprints posted at Preprints.org appear in Web of Science, Crossref, Google Scholar, Scilit, Europe PMC.

Copyright: This is an open access article distributed under the Creative Commons Attribution License which permits unrestricted use, distribution, and reproduction in any medium, provided the original work is properly cited.

Review

Hydroxyapatite as a Material for Transplantology: Clinical Experience and Prospects of Application

Vitaliy A. Markelov ¹, Kseniya V. Danilko ^{1,*}, Vadim A. Solntzev ¹, Svetlana V. Piatnitskaia ¹, Olga R. Shangina ², Azat R. Bilyalov ³, Svyatoslav S. Chugunov ³ and Iskander Sh. Akhatov ¹

¹ Institute of Fundamental Medicine, Bashkir State Medical University, Ufa 450008, Russia

² Federal State Institution "Russian Center for Eye and Plastic Surgery", Bashkir State Medical University, Ufa 450075 Russia

³ Institute of Digital Medicine, Bashkir State Medical University, Ufa 450008, Russia

* Correspondence: kse-danilko@yandex.ru

Abstract: The centrepiece of this analytical review is the metabolism of hydroxyapatite in its natural, bone, and synthetic forms, where the mitochondria-mediated mechanism may serve as the leading mechanism. The possibility that osteoblast mitochondria play an important role in the initial stages of bone mineralisation is discussed. Furthermore, the paper highlights the key role of mitochondria in the metabolism of synthetic hydroxyapatite. Differences between the results of in vivo and in vitro studies using synthetic hydroxyapatite of different morphologies are also detailed. It is noted that long-term infiltration with immune cells and in vivo studies are necessary to adequately evaluate hydroxyapatite as a bone-plastic material. Particular attention is given to the interaction of hydroxyapatite with immune cells and its ability to affect the ribosomes and mitochondria of cells. Due to its mechanical properties, scalability and potential use for the treatment of extensive bone defects of tumor origin, hydroxyapatite is a promising material. This study also highlights the importance of further development of in vitro research methods in the context of their biomimeticity. Overall, this work offers a theoretical direction for future studies of hydroxyapatite as a bone grafting material and emphasises the value of in vivo studies.

Keywords: hydroxyapatite; bone grafting; nanoparticles; immune response; mitochondria

1. Introduction

The basis of modern medical technologies aimed at bone tissue regeneration is the widespread use of grafts, the main component of which is hydroxyapatite. The diversity of grafts and their constituent materials used is an equal reflection of the extremely large variety of pathological conditions of bone tissue requiring the application of regenerative medicine technologies.

At the same time, the use of any grafts requires preliminary detailed analysis of the immune response in response to the introduction of this or that material. In this context, the unique properties of such materials as hydroxyapatites and their compositions [1,2], including exceptional phenomena in the context of immune response [3–5], become extremely important. In this regard, there is a need for a more detailed presentation of hydroxyapatites and their compositions as the main components for the fabrication of grafts to restore structural and functional pathologies of bone tissue.

Native form of hydroxyapatite: description of structure and functions in the body

First of all, it is necessary to note the fact that hydroxyapatite is the native form of bone tissue calcium and occupies 70–90% of the bone tissue matrix volume. In bone tissue hydroxyapatite is represented in the form of crystals of small size and is characterized by the stoichiometric formula $\text{Ca}_{10}(\text{PO}_4)_6(\text{OH})_2$ [6]. According to the age of a person, three main ranges of their average size are distinguished: up to 6 six years of age, 188–215 nanometers; between 6–19 years of age, 232–252 nanometers; and in adulthood, 252–283 nanometers [7]. Together with collagen I, which occupies up to 90% of the organic phase of bone, it forms the spectrum of the main structural and functional features of bone tissue [8].

The immediate beginning of the formation of the mineral component of bone tissue is provided by the energy-dependent movement of Ca^{2+} cations and serum phosphate ions into the mitochondria of

osteoblasts (Figure 1). When a solubility threshold is reached, micropackages of amorphous calcium phosphate or Posner clusters with the probable formula $\text{Ca}_9(\text{PO}_4)_6$ are precipitated, which are thought to be stabilized by an organic component, the so-called "Howard factor." Further release of amorphous calcium phosphate can occur in two ways: by direct transport directly across the mitochondrial membrane or by reverse phagocytosis [9].

The contents of vesicles initially form shapeless accumulations of calcium phosphate in dense association with collagen fibers. In the process of subsequent ion diffusion, rudimentary hydroxyapatite plates are formed, which in contact with each other sharply increase the degree of crystallization [10]. As a result, partly under the influence of noncollagen proteins [11–13], lamellar structures 2-4 nanometers thick are formed, the longitudinal axis of which is formed parallel to the axis of collagen fibrils (Figure 1) [6].

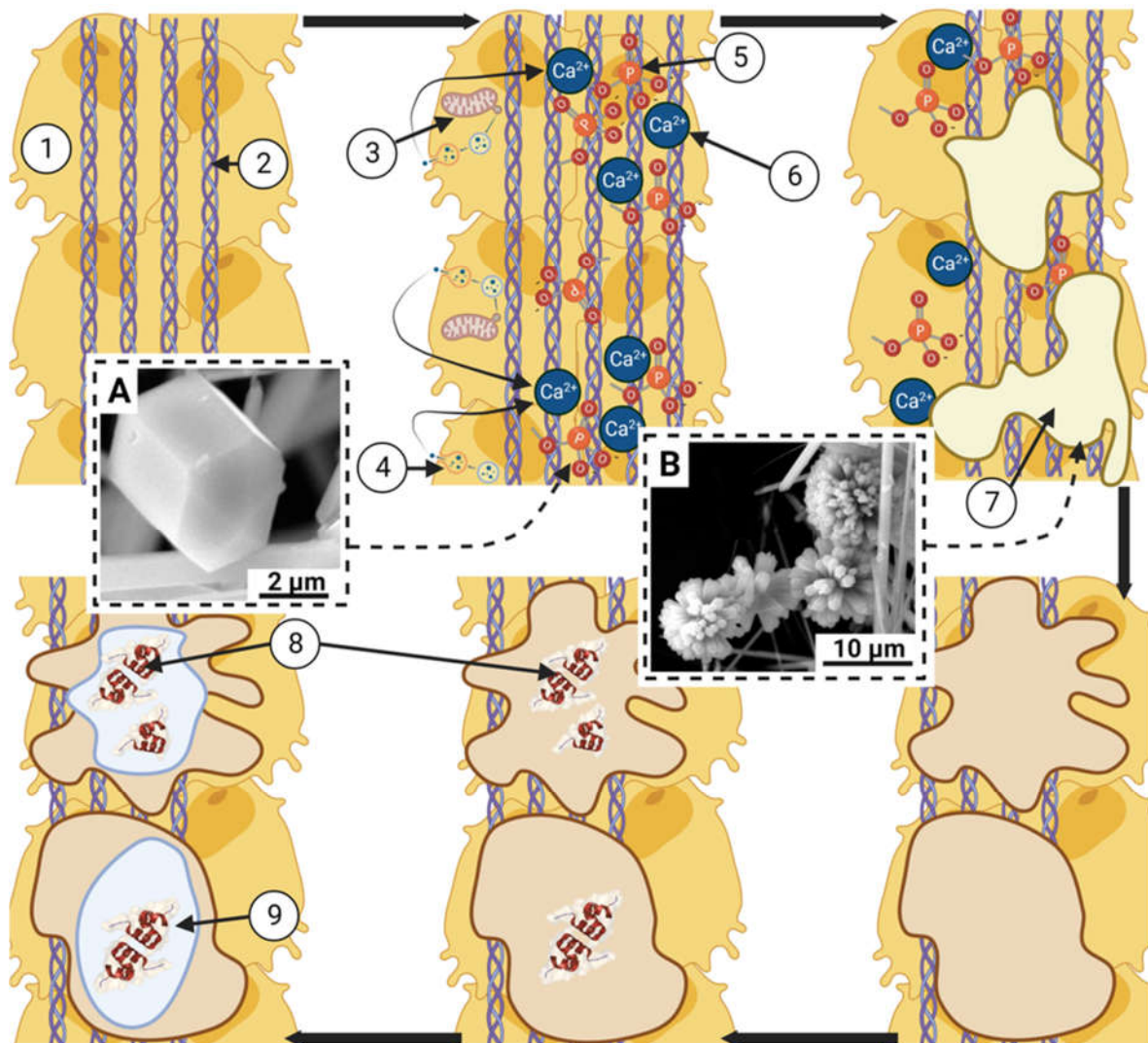


Figure 1. Scheme of the stages of collagen fibril calcification. 1 - osteoblasts; 2 - collagen fibrils; 3 - mitochondria of osteoblasts; 4 - microvesicular transport of calcium phosphate; 5 - phosphate (as part of still amorphous calcium phosphate); 6 - calcium (as part of still amorphous calcium phosphate); 7 - hydroxyapatite plates; 8 - osteocalcin; 9 - octacalcium phosphate; A - single hydroxyapatite crystal; B - group of hydroxyapatite crystals (microphotographs adapted from [14]).

Collagen fibrils act as an organizing component in the formation of growth centers of hydroxyapatite crystals [9,15]. The initiation of hydroxyapatite crystals formation depends on amino acid patterns, in particular, the triplet of amino acids glycine-proline-hydroxyproline, which is the dominant motif of tropocollagen. This process is caused by the formation of ionic bonds between calcium atoms, oxygen

atoms of carbonyl groups of the polypeptide backbone and side chains of proline and hydroxyproline [16]. If we consider a quasi-hexagonal model, lysine at position 108, glutamic acid at positions 110, 116, 582, and 815, and arginine at positions 350, 581, and 816 form a stereochemical pocket for optimal binding of calcium ions and phosphate ions [9]. The functionality of non-collagen proteins is largely due to the effect of osteocalcin. This protein plays a guiding role in the process of intrafibrillar appearance of hydroxyapatite crystals in type I collagen fibrils [17,18].

As a rule, bone tissue hydroxyapatite is carbonated with carbonate to some extent. The normal range of carbonate substitution is 2-9% [19]. Substitution by carbonate ions occurs at the positions of phosphate ions (PO_4^{3-}) (major B-type substitution) and hydroxyl groups OH^- (minor A-type substitution), thereby provoking a change in crystal structure and molar Ca/P ratio [19,20]. In the case of hydroxyl ion substitution, which is characteristic of bone apatite, a state of hydroxyl deficiency is formed, which has different degrees of severity depending on the type of bone tissue [21]. Subsequently, it increases the solubility of bone material [22].

As a consequence of this substitution, the mineral component of bone plays the role of the main depot of calcium, phosphorus, magnesium and a number of other mineral elements; this process has a high regulatory potential for the metabolism of these elements in the whole organism [19,23]. It is quite obvious that substitution by the mentioned elements affects numerous parameters of the crystal lattice. Iron and strontium have a positive effect on the dimensional characteristics of its individual elements, while zinc and magnesium have the opposite effect. For magnesium, zinc and iron a negative effect on the crystallinity of hydroxyapatite was revealed, for strontium - positive [23]. It is also noteworthy that the indicated effect of changing the crystalline microstructure of the mineral component demonstrates a striking heterogeneity in the composition of a single bone [24]. Relatively high strontium content is characteristic of regions with high metabolic activity and newly formed bone structures [25].

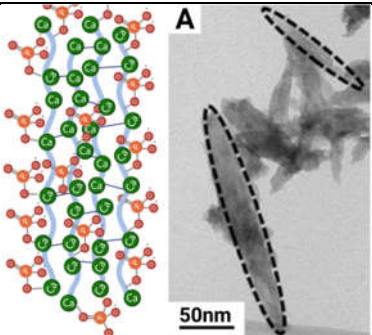
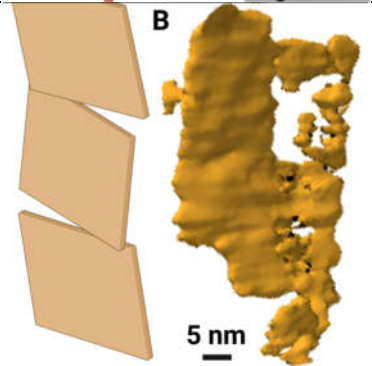
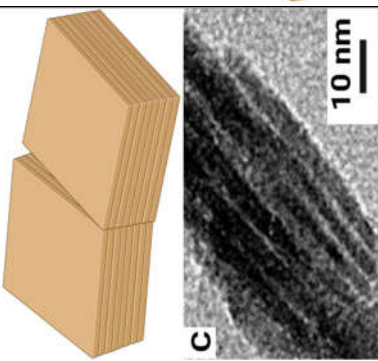
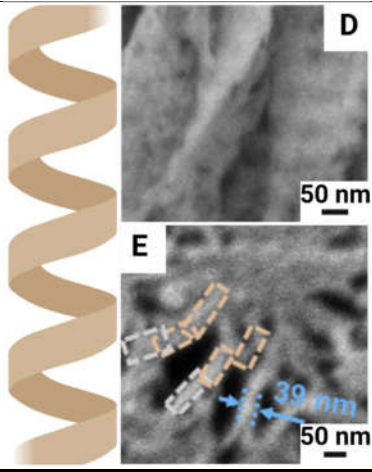
The most regular pattern of heterogeneity is the difference of surface and inner layers of hydroxyapatite. The surface layer is in the form of hydrated amorphous calcium phosphate 0.8 [19] or 1-2 nanometers thick [26] and a more crystallized core [19]. Hydroxyapatite is characterized by an extremely flexible microcrystalline structure, suggesting an extremely broad list of elements suitable as substituents. This may account for a wider and more localized range of possible biological properties of native bone hydroxyapatite.

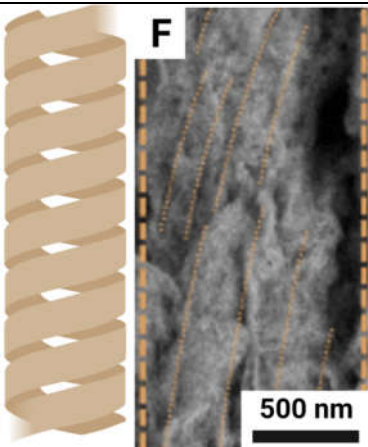
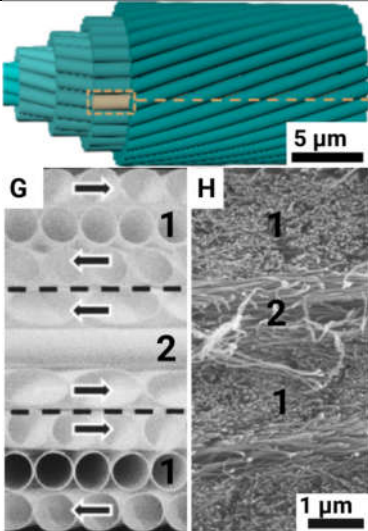
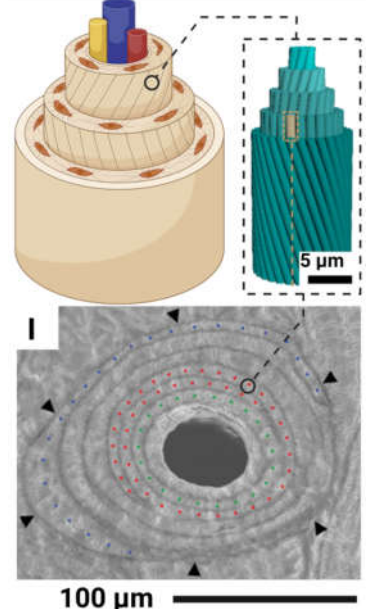
The fundamental reason for the structural strength and high resistance to ionic substituents is the hexagonal organization of hydroxyapatite [19]. However, in some cases, the loss of hexagonal structure and formation of monoclinic organization of the crystal lattice is possible [27], which largely depends on the degree of substitution of chlorine anion Cl^- [28]. Changes in the organization of the crystal lattice of hydroxyapatite are also possible as a result of age-related changes [29]. The observed lability has prompted a search for other constituents of the inorganic phase, such as tricalcium phosphate, dicalcium phosphate dihydrate [19] and octacalcium phosphate [30]. For the latter, no direct evidence has been shown for its presence in bone structure [19], except in pathological conditions [28] under relatively low pH conditions. However, there are studies that confirm the presence of a fixable amount of octacalcium phosphate in bone tissue under normal conditions [10].

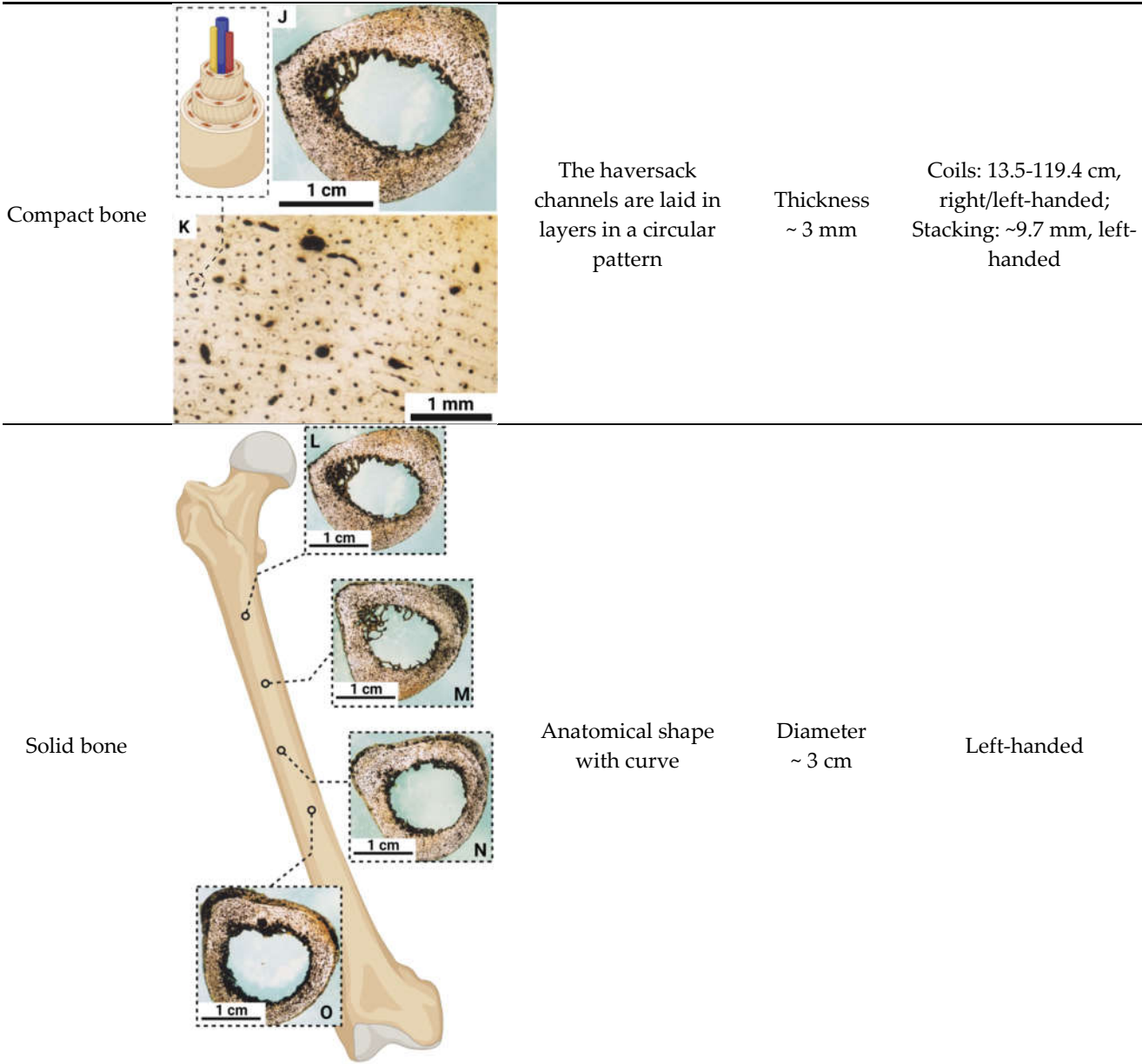
As for the higher-level organization of the mineral component of bone tissue, the formation of lamellar structures of hydroxyapatite is generally accepted [19]. Spirally twisted needle-like crystals of apatite, located within and between collagen fibrils [10,31], merge laterally and are organized in the form of spiral subplates along the loading axis. The defined chiral structure of the latter is the basis for tertiary helical plates. The further formation of the mineral base ordered in time and space with the formation of collagen structures results in a multilevel architecture of the inorganic component of bone [31]. The results of modern studies of the dimensional parameters of each level of organization of the inorganic component of bone are presented in Table 1.

Table 1. Hierarchy of bone tissue mineral component organization.

Hierarchy	Morphology	Size	Step length and chirality
-----------	------------	------	---------------------------

Needle crystal		Thin, twisted long ribbon	Thickness ~ 5 nm Width 5 to 10 nm Length 50-100 nm ~ 1.5 μ m right-handed
Subplate		Needle-shaped crystal merging laterally at an angle	Thickness 5 nm Width 20 to 60 nm Length 50-100 nm ~ 4.7 μ m left-handed
Plate		Twisted mineral laminae composed of subplates	Thickness 20-40 nm Width 60-150 nm Length 50-100 nm ~ 4.6 μ m left-handed
Mineral fibrils		Mineral plates spirally merge at an angle	Width 60-150 nm Length: Micron level ~ 2.9 μ m right-hand side

Bundles of mineral fibrils		Mineral fibrils spirally merge at an angle	Diameter 1-2 microns Length: Micron level	Coils: 4.2-6.5 μm right-handed
Lamellar units		The fibril bundles are rotationally stacked layer by layer	Diameter 6-12 microns	Coils: 48-653 μm , left/right; Stacking: ~47.6 μm , right-handed
Haver's canals		Lamellar units are spirally twisted around the blood vessel in the form of coaxial cylinders	Diameter 100-300 microns	Coils: 617-5,167 μm , right/left-handed; Stacking: ~184 μm , right-handed



Notes: A - transmission electron micrograph of Mg²⁺-doped needle microcrystal (adapted from [32]); B - model of a crowded mineral subplate formed by lateral fusion of needle microcrystals; C - transmission electron micrograph of twisted mineral plates, showing the stacking of subplates; D - scanning electron micrograph of spiral mineral fibrils, cross section; E - scanning electron micrograph of spiral mineral fibrils from a lateral perspective; F - scanning electron micrograph of spiral bundles of mineral fibrils from a side view (model and micrographs adapted from [31]); G - model of twisted plywood showing the ratio of transverse and longitudinal lamellae; H - scanning electron micrograph showing the alternation of transverse lamellae (1) and longitudinal lamellae (2) (model image and micrograph adapted from [33]); I - scanning electron micrograph showing the structure of the lamellar system: red dots display a closed ring structure; green dots display a spiral organization and overlap after a 360° turn; blue dots form a sickle moon structure and display an incomplete ring (adapted from [34]). J and K, cross section of the right femur at a distance of 14 centimeters from the proximal end; L, cross section of a horse femur stained with mercury sulfide, showing the arrangement of osteons in the repeat sheets of the capillary network; M, cross section of the right femur at a distance of 19 centimeters from the proximal end; N, cross section of the right femur at a distance of 23 centimeters from the proximal end; O, cross section of the right femur at a distance of 25 centimeters from the proximal end (photographs and microphotographs adapted from [35]).

Having analyzed a number of scientific studies of structural, physicochemical and physiological properties of the mineral component of bone tissue, we aim to emphasize the fundamental role of native

hydroxyapatite on the scale of the whole organism, defining it as the most valuable and convenient material in bone grafting. The spectrum of features of native hydroxyapatite presented in this section, beginning with the stoichiometric flexibility of the crystal lattice and ending with the complex process of its formation in the living organism, dictates completely new requirements for synthetic analogs of bone hydroxyapatite as a transplantation material. Among them the multilevel character of the organization, formed in close interaction with the organic component, including the cellular environment, stands out.

2. Hydroxyapatite as a bone grafting material

The generally recognized "gold standard" in bone grafting is the use of autologous bone material. Autologous bone grafting has been successfully used in clinical practice for a century [36,37]. This necessitates a comprehensive analysis of the main advantages of using this method in order to form a kind of reference heuristic model in the development and improvement of alternative sources of material for bone grafting. There is also a clear need to analyze the main problems of using autografts in order to use them in the formation of alternative solutions.

Starting from the reference value of bone autografts, we should define the attributes of an "ideal graft". First, it should possess the properties of autogenous bone, which include biocompatibility, osteoconductivity, and osteoinductivity. Second, the graft material should be easy to use, safe, and cost-effective [36].

The key conditions for successful bone tissue regeneration formulated in the "diamond concept" are worth mentioning from the generally accepted positions. Its essence is that successful healing of bone defects requires the presence of viable osteogenic cells or their precursors, a suitable connective tissue matrix, adequate vascularization, and a time- and space-specific profile of growth factors [38].

In this context, it is necessary to emphasize the main properties and the distribution spectrum of their values for bone grafts used in clinical practice:

1. The range of values of the structural parameter of the bone implant. Bone grafts have different ability to withstand mechanical loading. For unmodified grafts based on cortical bone a relatively high resistance to mechanical loads is shown in comparison with grafts based on cancellous bone. Thus, the mechanical properties of bone grafts without additional modification directly depend on the properties of the donor site [39].
2. Spectrum of osteogenic properties. The ability of the graft to initiate neoosteogenesis [40] due to the preserved pool of graft cells including osteoblast precursors [41] is extremely important. Due to the presence of cellular elements, necessary growth factors and matrix framework, such a graft is able to modulate angiogenesis, adequate perfusion [42,43] and activity of progenitor cells [44].
3. Osteoinductive properties. Autologous graft is characterized by the presence of an exhaustive set of growth factors necessary for regeneration, providing proliferative and differentiative potential of progenitor cells [45–47].
4. Osteoconductive properties. Ability to provide an optimal environment for normal metabolism, proliferation and differentiation of cell populations [48].

The material for autologous bone graft can be spongy or cortical bone. The advantage of the former is relatively high osteoconductive properties due to a significant concentration of osteogenic cells and growth factors. The main disadvantage of this type of graft is its low ability to provide structural support at the early stages of graft integration [36].

It should also be noted that despite all its undeniable advantages over alternative bone grafting strategies, the methodology of graft isolation continues to improve. A prime example of this is the use of femoral medullary bone chips obtained using the Reamer Irrigator Aspirator System (RIA - Synthes®, Inc. West Chester, USA) [49]. With equivalent rates of graft integration compared to traditional iliac crest harvesting, this method demonstrates a lower risk of chronic pain, infection, and excludes damage to the lateral cutaneous nerve of the femur as a result of compression or contusion [50]. However, the risk of complications such as cortical bone perforation and subsequent bleeding is still high [51].

Against this background, it should be emphasized that the autogenous cortical bone graft is also characterized to a greater extent by osteoconductive properties under the condition of lower biological activity compared to the spongy autologous graft. The next problem is the high duration of

revascularization [52,53]. For this reason, vascularized cortical grafting material that provides osteogenic and osteoconductive properties can be used [36]. In this direction, there is also a continuous development of strategies for the allocation of transplant material that ensure a reduction in the risks of donor site pathologies while maintaining the necessary integrative parameters [54]. However, the development of technologies takes place not only within the framework of improving the techniques of obtaining one or another type of autologous grafts separately. Of particular importance are the works in the direction of optimal combination of the presented types of transplant materials, which allows obtaining positive results, including in their clinical use [55,56].

Despite the benchmarks of autologous bone grafting material in the context of its osteogenic, osteoconductive, and osteoinductive properties, the number and variety of studies aimed at finding alternative strategies for graft preparation continue to grow. This is due to the fundamental disadvantages of all methods of obtaining autologous graft material: firstly, the limited volume of potential graft material [57,58]; secondly, the possibility of developing complications of the donor bone site [50,51]. Moreover, when taking autologous grafting material, the risk of bleeding increases, which still remains one of the main problems, including when using the latest methods of bone implant obtaining [51]. Thus, there are studies that confirm a significant incidence of complications both after traditional grafting from the anterior and posterior iliac crest (19.37%) and after using the Reamer Irrigator Aspirator system (6%). The general list of complications included the development of infection, hematoma, seroma, chronic pain, fracture, as well as vascular and nerve damage [59]. In a study conducted by Suda A.J. et al. it was shown that the volume of the removed transplant material has a great influence on the risk of serious complications [60]. Thus, we can say that the main limitation of autologous bone transplantation is the small volume of potential grafting material.

In this context, the development of a number of alternative methods for obtaining transplantation material is extremely important. This series includes obtaining allogenic [61–63] and xenogenic transplantation material of natural origin [62,64], as well as the creation of new biomimetic transplantation materials of artificial and bioengineered origin [62,65,66].

3. Native substitutes for autologous bone grafting material: allogeneic and xenogeneic bone grafts

Functionally, the closest of all the listed alternative methods is allogeneic grafting material. The main advantage of this material is its relatively high availability [67]. Therefore, it has been used in clinical practice for reconstruction of extensive bone injuries for many years. Like autogenous graft, allogeneic graft material has a high degree of similarity to the structure of native bone: it has similar mechanical properties, is biocompatible to a certain extent, and ultimately has osteoinductive and osteoconductive properties [63], which are limited [68], probably due to the need for decellularization of the graft material [63]. As noted by some authors, the key problems of this method are the lack of unified decellularization protocols and the potential risk of infectious disease transmission [68].

Conventionally, allogeneic bone grafts can be divided into two main groups. The first group includes various variations of allogeneic bone graft proper - decellularized bone graft of donor origin of one type. The second group includes demineralized bone matrices obtained by acid treatment of allogeneic bone graft in order to isolate bone collagen matrix [69]. It is important to note that there is an extremely wide range of methodological solutions to obtain allogeneic [70–72]. This, on the one hand, creates the problem of forming a unified protocol for wide implementation in clinical practice. On the other hand, it gives grounds for a personalized approach, which is actively used in clinical practice.

At the same time, demineralized bone matrix is an allogeneic bone material that was modified in accordance with the general provisions of the Marshall Urist technique [69]. It should be noted that this method, which has already become traditional, has undergone a significant number of modifications since its first use [73]. For example, the preparation of commercial demineralized bone matrix has wide limits of variability among different manufacturers, including the use of different acid solutions, changes in the duration of demineralization, different temperature regimes and methods of decontamination [74,75].

In comparison with autologous grafts, allogeneic transplant material demonstrates some characteristic features. The common property, which directly depends on the main stage of obtaining all allogeneic grafts - decellularization, is the absence of pronounced osteogenic properties [69,76]. Nevertheless, according to

the "diamond concept" [38], allogeneic bone grafting material has high osteoconductive and osteoinductive properties.

A certain degree of bone allograft effectiveness in clinical practice is largely due to its osteoconductive properties and high value of mechanical support [69] in bone injuries requiring a large volume of grafting material [77,78]. As in autologous transplantation, the most pronounced osteoconductive properties are characteristic of the allograft of cancellous bone [36]. The variability of the content of osteoconductive agents in the final graft material is largely due to the duration of storage and preparation conditions [79,80].

Taking into account the facts stated in the conclusion of the previous section, we need to focus our attention on clinical practice. As it has already been mentioned, the main indication for the use of allogeneic grafting material is extensive bone tissue damage requiring a significant volume of grafting material [81–83]. The time interval of allografting is of particular importance in this context. Since this type of transplant material, despite decellularization [84], has a relatively high frequency of immunogenic rejection [85]. At the same time, in case of extensive bone injuries, including those caused by infectious agents [86], there may be an immune hypersensitivity reaction to an allogeneic graft due to already existing inflammation [69]. Therefore, in clinical practice, the strategy of delayed bone grafting (after 6-8 weeks after the primary surgery) is often used [86,87].

The current trend in the use of allogeneic bone grafting material is the use of cellular bone matrices. The essence of this method is the implantation of allogeneic mesenchymal stem cells into the structure of the osteoconductive and osteoinductive base. The cellular component is obtained by isolating multipotent stromal cells from cadaveric bone marrow, adipose tissue, and chorion tissue [88]. However, some authors speak about the controversial efficiency of their use [89].

A combination of allogeneic and xenogenic bone grafting materials can also be used, where the former performs the role of an osteoinductive agent and the latter performs a mechanical role [90]. The category of xenogenic bone grafts should be noted separately: bovine bone material is often used for their production [91–93]. There are data confirming high osteoconductive properties of xenogenic bovine bone material [94], while the independent use of xenogenic bone grafting material, despite the positive postoperative outcome in individual cases [95], demonstrates poor quality of clinical outcome [96,97]. The main negative results of xenotransplantation are fibrous encapsulation of the graft [98] and improper fusion, which is manifested by pain syndrome [99]. Moreover, due to the extremely high duration of xenograft integration (57 weeks) compared to allograft (16 weeks), many researchers have decided that xenografts should not be used independently [96].

Summarizing the data presented in this section, it is worth noting that, on the one hand, the direction of allogeneic transplantation material use is constantly replenished with original methods, including the use of additional categories of transplantation materials. However, on the other hand, in this area there is a noticeable problem with the standardization of the existing methodological base [100]. In clinical practice, this leads to the need to use strategies of personalized medicine, limiting the prevalence of application.

4. Semisynthetic and synthetic bone substitutes

Considering the data presented in the previous sections, we need to pay special attention to the possibility of increased risk of transmission of infectious agents by transplantation of allogeneic [101,102] or xenogeneic [103] grafting materials. It is also necessary to consider the high risk of developing an increased immune response in allogeneic bone grafting [104,105], as well as the negative results of the integration of xenogenic bone grafting material [96–99]. The presented difficulties in the use of allogeneic and xenogenic bone grafts create the need to develop safer, affordable and comparably effective alternatives.

In the sections above, strong evidence has already been presented for the feasibility of using hydroxyapatite as a basis for synthetic compositions and materials that can potentially have all the required properties as an alternative to autologous grafts. This is also supported by the use of hydroxyapatite bioceramics in current clinical practice in solid, granular, powdered, porous and composite forms [106–109]. The latter form attracts special attention because being native bone tissue, bone autografts are composites [110,111].

There are two main categories of methods of hydroxyapatite production, dry methods and solvent methods [112]. Dry methods are characterized by the use of mechanical action and high temperatures. The schematic order of this method is shown in Figure 2.



Figure 2. Schematic representation of the simplest algorithm of the dry method of hydroxyapatite production. 1 - source of calcium raw material (calcium hydroxide or calcium acetate monohydrate); 2 - source of phosphates (phosphorus pentoxide ammonium hydrophosphate); 3 - optional introduction of various salts, most often magnesium salts; 4 - pre-prepared calcium phosphate powders can also be used; 5 - intensive mechanical grinding (vibrating ball mill); 6 - high-temperature treatment of the powder mixture; 7 - transfer material in the form of primary raw material (adapted from [113]).

In this process, the precursor is first pulverized and heated at a very high temperature of 1000°C [114]. These techniques do not require the use of solvent [113]. In particular, a mixture of tricalcium phosphate [$\text{Ca}_3(\text{PO}_4)_2$ or $3\text{CaO} \cdot \text{P}_2\text{O}_5$] and tetracalcium phosphate [$\text{Ca}_4(\text{PO}_4)_2\text{O}$ or $4\text{CaO} \cdot \text{P}_2\text{O}_5$] can be used. In general, the solid-phase production of hydroxyapatite results in a well crystallized product [112,115]. The quality of the raw materials obtained in this way is not significantly influenced by processing factors. This creates the basis for large-scale production [116,117]. However, hydroxyapatite obtained by this method often exhibits phase heterogeneity [118]. There is a variation of the solid-phase method that produces more homogeneous hydroxyapatite, the mechanochemical method. However, this modification is not able to sufficiently improve phase heterogeneity [113]. Moreover, hydroxyapatite obtained by this method has low biomimetic properties, which makes it necessary to analyze alternative methods of hydroxyapatite production [119].

Chemical precipitation method: based on a category of methods for the production of hydroxyapatite using different solvents for chemical precipitation of various sources of calcium (calcium nitrate $\text{Ca}(\text{NO}_3)_2$) and phosphate (diammonium dihydrophosphate $(\text{NH}_4)_2\text{HPO}_4$) [112] in the presence of a wide variety of substituents [120–123] in acidic or basic media. The range of conditions for conducting the co-chemical precipitation is highly variable. The pH values vary from 3 to 12 [112,124]. The temperature regime of the reaction has an extremely wide range [112,125]. The schematic algorithm of this method is presented in Figure 3.

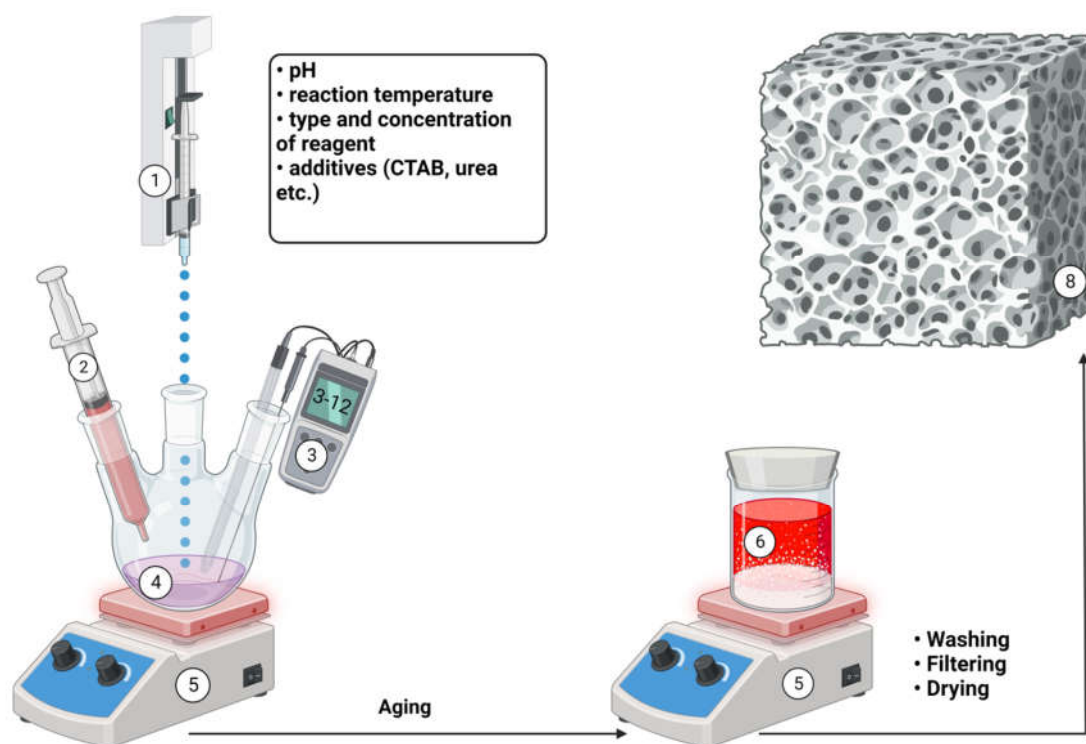


Figure 3. Schematic representation of the algorithm of hydroxyapatite fabrication by chemical precipitation. 1 - syringe pump with reagent containing Ca^{2+} cations, most often calcium nitrate ($\text{Ca}(\text{NO}_3)_2$); 2 - Ph-controller (often ammonium solution); 3 - Ph-meter (control of Ph-reaction mixture); 4 - reagent containing phosphate-anions (most often diammonium phosphate $(\text{NH}_4)_2\text{HPO}_4$); 5 - stirring and temperature control using a heated magnetic stirrer; 6 - precipitation of hydroxyapatite particles; 7 - transfer material in the form of primary raw material (adapted from [113]).

In contrast to dry methods, solvent-based technology results in hydroxyapatite particles with a more biomimetic morphology. Equally important is the ability to manipulate particle size and morphology given the relative simplicity of the technology [113]. As a result of this reaction, it is possible to produce spherical and needle-shaped hydroxyapatite nanoparticles [126], which are native forms of bone hydroxyapatite [31]. By this method, it is possible to obtain hydroxyapatites with the desired ionic substitution of the crystal lattice for magnesium [120], strontium and lithium [127], manganese, thereby regulating the degree of carbonization [121], aluminum [122], zinc [127,128], selenium [123], various rare earth metals [129] and a number of other elements, including copper and silver [130].

Along with the use of substitute agents for the components of the hydroxyapatite crystal lattice, the co-chemical deposition method is often used for its synthesis in relatively pure form [131] or in the form of multilevel compositions using additional materials in a variety of ratios and forms. Examples include coatings for substrates made of polymeric [132–134], metallic [135,136] or combined compositions [137,138]. Also composite porous micelles [139], composite hydroxyapatite nanoparticles [140] and hydroxyapatite nanotubes [141] or nanorods [142] can be obtained by this method.

Nevertheless, for hydroxyapatite obtained by chemical precipitation method, it is often found that the required stoichiometric parameters are absent. And, in contrast to dry production techniques, the raw materials obtained by chemical precipitation have low crystalline parameters [113]. Thus, as in the previous example, the need for further consideration of alternative methods of obtaining hydroxyapatite becomes obvious.

Electrochemical deposition method: widely used for the synthesis of biomedical coatings and membranes. There are two main categories of electrochemical method performance: electrophoretic process - based on the use of a suspension of ceramic particles; electrolytic process - based on the use of metal salts. The material for this method is aqueous solutions identical to those used in chemical precipitation [143]. This method is characterized by such positive features as the speed of formation of a

uniform coating at relatively low temperatures. Electrochemical methods provide good impregnation of hydroxyapatite into the composition of porous substrates and carriers, resulting in the formation of a uniform and durable coating [143,144]. This was greatly facilitated by the introduction of the pulsed electrodeposition method, which reduced the release of hydrogen gas bubbles during the electrochemical reaction [143]. As in the case of chemical deposition, the electrodeposition method is used to create composite structures of hydroxyapatite with a wide variety of morphologies. These include composite coatings, including aluminum-containing coatings [145], for a variety of alloys [146–148] including aluminum alloys [149], and for some polymer implants [150]. The mentioned range of morphological diversity also includes hydroxyapatite nanotubes [151] and hydroxyapatite nanoparticles [152]. However, most commonly, nanoparticles, microparticles and other dispersed forms of hydroxyapatite are used as drug delivery agents [129,153,154].

Emulsion method: one of the most effective methods for obtaining nanostructured hydroxyapatite powder formed in a dispersed medium of two immiscible solvents. This medium is stabilized by surfactants. It is most often used as a method for efficient production of composite materials using finished hydroxyapatite particles.

The method of producing the emulsion is largely determined by the concentration and nature of the surfactant introduced [155]. Agglomeration creates a favorable environment to regulate particle growth. Hydrophobic surfactants are subsequently easily removed by calcination [156].

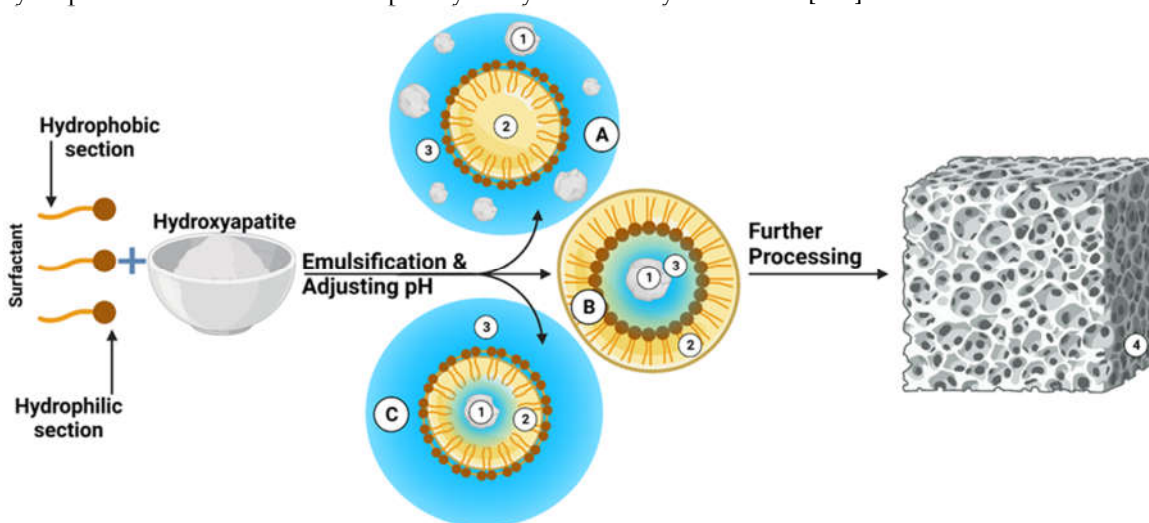


Figure 4. Schematic representation of the algorithm of hydroxyapatite fabrication by emulsion method. 1 - hydroxyapatite particles; 2 - oil phase; 3 - aqueous phase; 4 - transfer material in the form of primary raw material; A - oil encapsulated in aqueous phase containing particles; B - oil encapsulates aqueous phase with hydroxyapatite particle; C - emulsion system where aqueous phase contains oil droplets with encapsulated aqueous medium containing hydroxyapatite particle (adapted from [113]).

Its advantage is the strict control of morphological and dimensional parameters of nanoparticles. Due to this method is often used to create porous materials, acting as a solution to some difficulties in the agglomeration of hydroxyapatite particles. As sources of calcium and phosphate it is possible to use available precursors: calcium nitrate and phosphoric acid. The surfactants used to prepare the emulsions are sodium dioctyl sulfosuccinate, dodecyl phosphate, polyoxyethylene, non-polyphenol ether, polyoxyethylene ether, cetyltrimethyl ammonium bromide and sodium dodecyl sulfate. In addition to the characteristics of the surfactant, the ratio of aqueous and organic phases, pH, temperature regime and the concentration of calcium and phosphate sources have a special influence on the final performance of hydroxyapatite obtained by the claimed method [112].

Sol-gel method: This method is one of the most popular methods for obtaining hydroxyapatite from a solution of preferably organometallic precursors [158]. It is convenient for obtaining film coatings [159,160] and aerogel structures of hydroxyapatite [112]. In the most general sense, this process involves hydrolysis of precursors to form micelles associated with templates in aqueous or organic media. This provides high chemical homogeneity of the resulting material [161], suitable stoichiometrically, high available surface

area, and minimal dimensional clustering. With all this, this method does not require high temperatures [162]. The results of in vitro studies also confirm the advantage of the material obtained by this method in terms of bioresorbability compared to the results of alternative methods [113]. Despite the unique properties of the materials produced by this method, this method has limitations in terms of scalability. The main reason for this is the high cost and scarcity of alkoxide-based precursors and the need for extremely fine control of the production process. Inadequate control of the production process is often responsible for the formation of secondary phases in the form of CaO , $\text{Ca}_2\text{P}_2\text{O}_7$, $\text{Ca}_3(\text{PO}_4)_2$ and CaCO_3 [112].

It is also not uncommon to observe the introduction of combined production technologies involving the use of several methods. Thus, the product of the emulsion method is subjected to high-temperature treatment [156]. High-temperature processing methods such as pyrolysis provide stoichiometrically pure and very crystalline hydroxyapatite powders [113]. This allows its use as a final step in the fabrication of hydroxyapatite material in order to increase the crystallinity of the raw material for graft fabrication [157]. However, this method can also be used as an independent method of hydroxyapatite production. There are two main variations of this technology - the method of pyrolytic spray and the method of pyrolytic spraying. In the first case, a pre-prepared solution of calcium and phosphorus salts is sprayed into a high-temperature furnace. As a result, water evaporates and the remaining particles crystallize to form hydroxyapatite. In pyrolytic spraying, a dense and durable coating of hydroxyapatite is formed on the target surface. In both cases, the morphology and size of the particles directly depend on the similar characteristics of the sprayed and sputtered droplets, which allows controlling these characteristics [113]. The schematic algorithm of this method is presented in Figure 5.

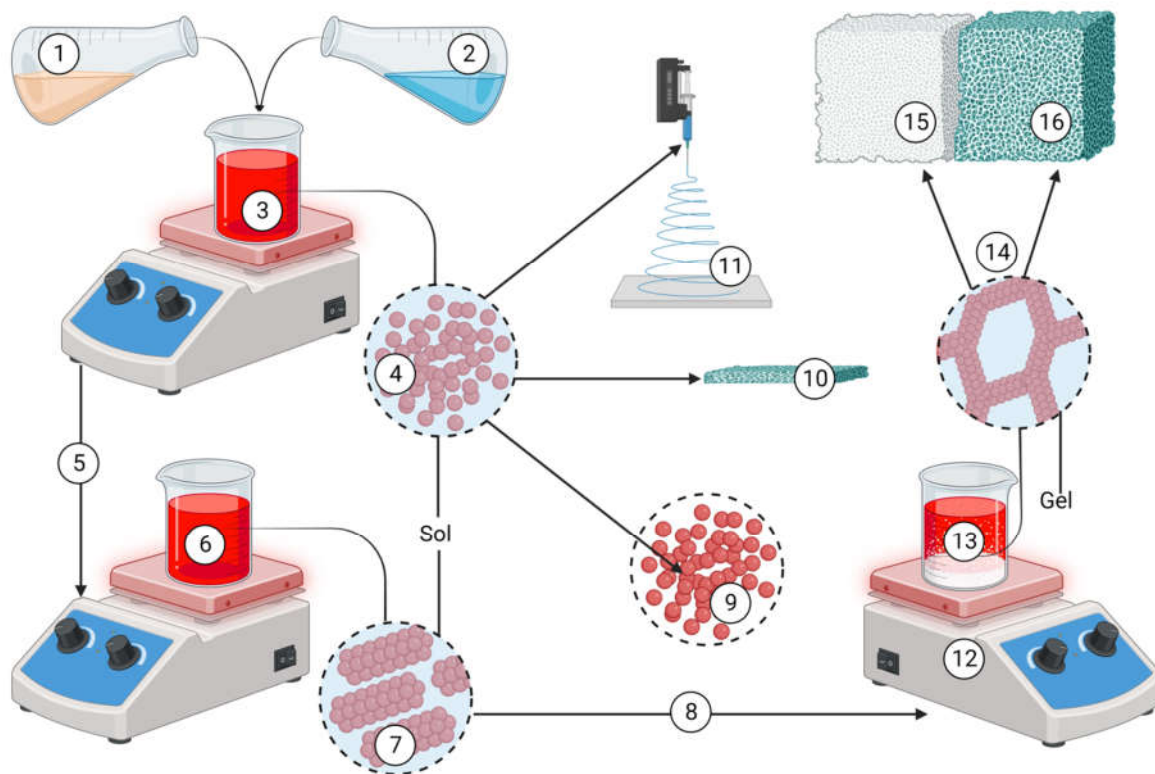


Figure 5. Schematic illustration of sol-gel method of hydroxyapatite production. 1 - phosphate-containing reagent (phosphorus pentoxide, ammonium hydrophosphate or triethyl phosphate); 2 - calcium-containing reagent (calcium nitrate, calcium acetate monohydrate or calcium ethoxide $\text{C}_4\text{H}_{10}\text{CaO}_2$); 3 - solvent (water or ethanol), control of reaction of sol formation; 4 - sol state of reaction mixture; 5 - transition of reaction mixture from sol to gel; 6 - control of coagulation reaction parameters; 7 - coagulation; 8 - direct transition to gel formation state; 9 - deposition with formation of material in powder form (individual particles); 10 - formation of coatings; 11 - formation of ceramic fibers as a result of electrospinning; 12 - control of gel formation reaction conditions; 13 - gel; 14 - evaporation and solvent extraction; 15 - formation of aerogel; 16 - dense ceramics (adapted from [112]).

Special attention should be paid to the methods of hydroxyapatite production from biogenic sources, the main examples of which are presented in Table 2. The most popular raw material for this method of hydroxyapatite production is the use of various biological wastes: bovine bone mass [163,164], eggshells [165,166], marine organisms [167–170] and plant materials. The latter can be used to extract hydroxyapatite per se [171] as a solvent [172,173] or as a source of calcium [174] and as a source of phosphate [175,176]. Moreover, the possibility of using plant-mediated synthesis of nanostructured hydroxyapatite for medical use has been shown [177]. It is important to note that some fungi possess the ability to synthesize nanostructured hydroxyapatite [178]. This may indicate their use as potential agents of hydroxyapatite synthesis for the needs of transplantology.

Table 2. Utilization of different biogenic raw materials of hydroxyapatite.

Source	Extraction method	Final product	Results of <i>in vitro</i> and <i>in vivo</i> studies	Ref.
Cattle bone waste	Calcination without chemical agents.	Hydroxyapatite nanoparticles with good crystallization are hexagonal in size 300-500 nm.	In vitro cytocompatibility studies have shown high rates of cell viability and proliferation when co-cultured together	[164] [187]
Horse bone waste	Sintering and processing in ball mill	Hydroxyapatite nanoparticles of two size groups: ≤ 500 and 200 nm.	High ability to induce osteogenic differentiation of dental stem cells	[188]
Fish waste <i>M. furnieri</i>	Treatment with NaOH and H ₂ O ₂ and calcination at 800°C	Hydroxyapatite powder with well-crystallized structure. Hydroxyapatite particles with pore size ~8 μm.	Collagen fiber formation, fibroblasts were present and angiogenesis was observed. Tissue proliferation into the graft was observed.	[167] [189]
Bone waste of <i>Hypophthalmichthys molitrix</i>	Treatment with NaOH and acetone	Hydroxyapatite powder with an average crystallite size of 58.3 nm.	Cell viability of osteoblast-like MG63 cells is 91%. Positive effect on differentiation and proliferation.	[190]
	Tempering at 900°C	Hydroxyapatite powder with an average crystallite size of 64.3 nm.	MG63 cell viability is 86%. Low indicators of proliferative capacity.	
Tilapia bone waste	Tempering in the temperature range from 600°C to 800°C	Hydroxyapatite grains with a distinct porous structure and a relatively high degree of Mg ²⁺ substitution.	High degree of biocompatibility. Promotes cell proliferation and differentiation compared to commercial pure hydroxyapatite.	[186]
Bone waste from <i>E. chlorostigma</i>	Alkaline hydrolysis and calcination at 600°C	Nanoscale hydroxyapatite measuring 29.5 nm for alkaline treatment and 82.12 nm for calcination	High biocompatibility of normal adipose fibroblast L929 cells. High proliferation L929. High remineralizing potential.	[191]
<i>L. catla</i> and <i>N. japonicus</i> scales.	Tempering at 800°C and grinding in a bead mill	Hydroxyapatite in the form of nanopowder of porous nanoparticles of size 30-60 nm with crystallites of size 10 nm.	When used in conjunction with the polycaprolactone scaffold, proliferation and excellent adhesion rates were observed	[170]
<i>L. lentjan</i> scales	Hydrothermal treatment at 280°C	Hydroxyapatite in the form of rods 50-100 nm long, 8-12 nm in diameter, and spheroids with a diameter of 15-50 nm	Biocompatibility and osteogenic potential for human mesenchymal stem cells.	[192]
Plankton	Leaching of solid particles	Porous nanohydroxyapatite	Adhesion, proliferation and viability. Increased expression of bone morphogenetic protein 2, collagen-1, osteocalcin and sialoprotein.	[193]
<i>Atactodea glabrata</i> shells	Tempering and chemical precipitation	Hydroxyapatite powder in the form of nanoscale rods 15.22 nm	Absence of cytotoxicity. Inhibitory effect against some pathogenic bacteria and fungi.	[168]
<i>Sepia</i> cuttlefish skeleton	Hydrothermal treatment with NH ₄ H ₂ PO ₄	Hydroxyapatite microspheres 1-2 microns in size with a trace element content close to human bone	Absence of cytotoxicity of MG63 cells. MG63 proliferation. High alkaline phosphatase activity and osteocalcin expression.	[194]
<i>A. fulica</i> shell	Tempering. Sintering with (NH ₄) ₂ HPO ₄ .	Nanoparticles of hydroxyapatite with the size of 87.7-88.9 nm	Distinct antibacterial activity	[195]
Eggshell	Hydrothermal acid treatment with H ₃ PO ₄ .	Single-phase crystalline hydroxyapatite (26.5, 40.8 and 25.5 nm) with high Mg and Sr content.	High adhesion of MG63 cells. The cells had distinct filopodia.	[165]

The main requirement for this type of feedstock is the removal of organic matter, which can be achieved by temperature treatment per se [165] and by using subcritical water [179,180]. The use of alkaline thermal hydrolysis [180] and enzymatic treatment methods [181] and so on are also commonly practiced.

As mentioned in previous sections, the most obvious difference of biogenic hydroxyapatite is the strong stoichiometric diversity. Natural hydroxyapatite has different degrees of substitution in elements such as Na^+ , Zn^{2+} , Mg^{2+} , K^+ , Si^{2+} , Ba^{2+} , F^- , and CO_3^{2-} [19,182]. This accounts for the diversity of functions of natural hydroxyapatite as an element of bone tissue. A more detailed description of each function is given in the previous structural sections. Table 2 summarizes the results of recent studies. These data, in addition to the high feasibility of using this raw material, give an idea of the high degree of biomimetic potential of the obtained hydroxyapatite in comparison with the mineral phase of human bone [165]. This is supported by the data that testify in favor of similarity of leading morphological and microarchitectural parameters of treated hydroxyapatite, including agglomeration of hydroxyapatite particles as a result of high-temperature treatment [183]. For example, the specific surface area of synthesized hydroxyapatite is in the range of values typical of native bone tissue [184]. This method results in a material with native porosity [185,186]. This is largely responsible for high indicators of biocompatibility, adhesive and osteogenic activity, which is clearly reflected in modern studies (presented in Table 2).

There is also a whole range of alternative methods for the production of hydroxyapatite using a wide variety of synthetic precursors, these methods are often based on identical mechanisms. Nevertheless, we can say with full confidence that there is no lack of diversity in the methods of synthetic hydroxyapatite production, which are determined by the variety of required characteristics and conditions of application of the final graft. In turn, the diversity inherent in synthetic methods of hydroxyapatite production determines the popularity of its application in research and clinical practice.

Semi-synthetic and synthetic bone substitutes in research and clinical practice

The vast majority of grafts used in bone regeneration are temporary scaffolds and provide structural support, promote bone repair and guide bone growth. Note that designing such a framework is a critical task. As semi-synthetic and synthetic grafting materials provide targeted modifiability, consistency and coherence as well as better availability. For example, one study confirmed the extremely positive dynamics of new bone formation based on hydroxyapatite scaffold populated with human bone marrow stromal cells [196].

Among the most popular representatives of synthetic bone substitutes, the group of calcium-phosphate ceramics, which includes hydroxyapatite, including its various modifications, beta-tricalciumphosphate and alpha-tricalciumphosphate and calcium sulfate, as well as various bioactive glasses and polymers, is particularly notable [197].

In comparison with other representatives of popular synthetic bone substitutes, hydroxyapatite has a number of features: relative to beta-tricalcium phosphate, carbonate apatite, which is considered as a modification of hydroxyapatite [198,199], has increased solubility in conditions that mimic Hauschip lacunae or resorption fossae [200]. Depicted in Figure 6. The latter structures are the result of osteoclast activity and play an important role in the bone remodeling process [201]. The aforementioned may indicate a more targeted response of this material in the format of natural bone remodeling, which may result in a relatively high osteogenic potential. While resorption of beta-tricalcium phosphate is maximal under physiologically normal conditions [200]. For alpha-tricalcium phosphate, even higher resorption under physiological conditions and the ability to rapidly hydrolyze to calcium-deficient hydroxyapatite have been shown [202].

In comparison with calcium sulfate (calcium sulfate semihydrate), magnesium substituted hydroxyapatite showed low resorption when transplanted into human bone defects [203]. At the same time, a more intense, incomplete osteogenic response was observed for calcium sulfate compared to the response to beta-tricalcium phosphate/apatite transplantation [204].

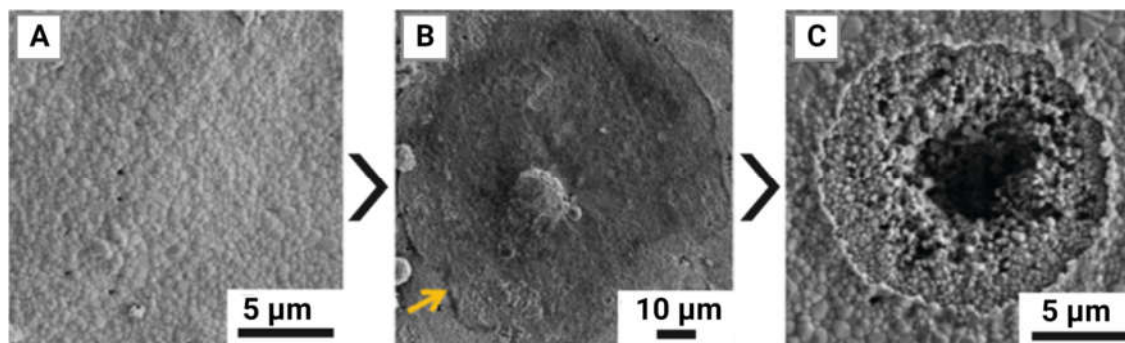


Figure 6. Hauschip's lacuna or resorption fossa, scanning electron micrographs: A, micrograph of cell-free hydroxyapatite surface with mean particle size 476.70 ± 100.71 nm; B, osteoclast (yellow arrow) on hydroxyapatite surface with mean particle size 476.70 ± 100.71 nm; C, resorption fossa on hydroxyapatite surface with mean particle size 476.70 ± 100.71 nm formed by osteoclasts (adapted from [205]).

When comparing hydroxyapatite and bioactive glasses, which are a group of synthetic materials based on silicon dioxide, calcium and sodium dioxide, it is necessary to note distinct osteoconductive properties [197]. This feature of this material is due to the formation of an amorphous layer on its surface, where favorable conditions for the concentration of structural proteins and growth factors are formed [206]. A comparative analysis of grafting materials based on hydroxyapatite, bioactive glass, and composites containing both materials showed an increase in osteoconductive potential when hydroxyapatite was added [207]. Thus, for amorphous bioglass 45S5 Bioglass® in in vivo studies a tendency to implant fracture was revealed [207,208]. This, to a certain extent, is also solved by the inclusion of hydroxyapatite in the composition of grafting material based on bioactive glass [207].

Also, when comparing the results of hydroxyapatite and bioactive glass transplantation into the defect of rat calvaria for the first material, a significantly more voluminous area of newly formed bone, as well as a significantly higher content of tartrate-resistant acid phosphatase (TRAP)-positive cells are noted [209]. The latter are more represented by osteoclasts and macrophages [210,211]. Together with the data on the comparatively better response of hydroxyapatite to the conditions of native remodeling [201], the above suggests a special relationship between hydroxyapatite and its derivatives and osteoclasts as derived monocytic precursors.

With regard to polymeric synthetic bone substitutes, there is also a tendency to increase osteogenic potential when hydroxyapatite is included in their composition. This phenomenon may be due to the intensification of osteoblastic differentiation when using polylactide and polylactide-co-glycolide [212]. When using a polyurethane composite with the addition of 40% hydroxyapatite, a significant increase in biomineralization capacity and osteogenic differentiation of mesenchymal stem cells in in vitro assays and the formation of a noticeable volume of vascularized bone tissue in in vivo studies were noted [213]. A similar trend is characteristic of polyethylene glycol diacrylate-based grafting material. The inclusion of hydroxyapatite into the material composition markedly increased the mechanical properties and biocompatibility of the prepared grafts in comparison with pure polymeric grafting material [214]. This trend is confirmed in the vast majority of cases of joint use of synthetic polymers and hydroxyapatite for bone grafting [215].

The above data allow us to speak about the interaction of hydroxyapatite with TRAP-positive cells, including osteoclasts and their immune precursors, as one of its key features in the role of bone grafting material. Thus, there is a clear need for a more detailed analysis of the literature data on the interaction between this transplant material and the recipient's immune system. The role of mononuclear phagocytic series is of particular importance in this context.

5. Interaction between mononuclear phagocytic cells and hydroxyapatite-based transplant material

One of the earliest literature reports of a direct relationship between hydroxyapatite and a distinct, acute, immune response, is a study of aseptic destruction and osteolysis of bone tissue in response to the use of hydroxyapatite as a bone grafting material. The occurrence of this reaction was found to be directly dependent on graft wear particles smaller than 53 μm . The results of the study demonstrate the ability of hydroxyapatite of this size to reduce the number of viable osteoblasts and activate osteoclasts [216]. Apparently, this effect of small-sized hydroxyapatite is characteristic for a wider range of cells and especially for cancer cells. When internalized in them, hydroxyapatite particles suppress their proliferation by inhibiting protein synthesis, blocking the availability of ribosomes for mRNA [217]. As well as the previous example, the data of comparative analysis of synthetic bone substitutes presented in the section "Semisynthetic and synthetic bone substitutes in research and clinical practice" confirm the possibility of using this feature of hydroxyapatite in clinical and research practice.

Less than 10 years later, data were obtained that directly confirm the ability of hydroxyapatite to initiate differentiation of macrophages toward an osteoclast-associated phenotype. Monocytes were characterized by the formation of a flattened phenotype with an irregular cell shape. Monocyte-macrophage cells were characterized by a marked increase in receptor activator of nuclear factor kappa-B ligand (RANKL) expression (modulates osteoclast activity) and formation of peripheral podosome belt [218] - dynamic actin and membrane-bound microdomains formed as an interconnected network of cytoskeletal units, forming a cytoskeletal superstructure in association with the plasma membrane [219].

In the context of literature data that demonstrate the ability of nanostructured hydroxyapatite to inhibit protein synthesis [217], it is extremely interesting that monocytes in the presence of hydroxyapatite showed signs of protein synthesis intensification [239]. At the same time, nanosized hydroxyapatite is able to initiate selective apoptosis of rabbit squamous VX2 tumor cells [220], growth inhibition of melanoma [221] and other types of tumor cells. This is primarily due to disruption of cellular calcium homeostasis and activation of endogenous mitochondrial and activation of external apoptosis stimuli [153].

Hydroxyapatite pretreated by partial dissolution and precipitation showed a markedly larger area of TRAP-positive staining (increased osteoclast activity) and increased expression of osteoclast-related genes compared to standard hydroxyapatite. The researchers attribute this difference to the presence of nanoscale hydroxyapatite particles in the treated material, while a homogeneous coarse-grained structure has been shown for standard material [222]. This work demonstrates the critical role of nanostructure and microstructure of hydroxyapatite, which is in good agreement with the fact that a lamellar microstructure is associated with a higher proliferative capacity of cells in the early stages of co-incubation. On the contrary, for hydroxyapatite with needle-shaped nanostructure, a noticeable increase in the number of cells is noted only in the late phases of the experiment. Also, for the former, a greater number of bound macrophages with flattened morphology is noted [223]. The following work extends the understanding of this phenomenon. First, strong evidence was obtained in favor of the effect of hydroxyapatite particle morphology on cytokine production by mouse dendritic cells. The highest rates of interleukin 1 β (IL-1 β) secretion were detected in response to needle-shaped hydroxyapatite, while the ability to significantly increase IL-1 β synthesis was not detected for smooth particles ~100 μm in size. For smaller spherical particles, a significantly lower ability to produce IL-1 β by murine macrophages was detected. The maximum expression of IL-1 β by murine macrophages was detected in response to needle-shaped hydroxyapatite particles. Expectedly, they also induce significantly higher inflammatory responses upon intraperitoneal injection compared to their spherical counterparts. For mouse peritoneal exudate cells (CPEM) stimulated with ~5 μm needle-like hydroxyapatite particles, higher levels of tumor necrosis factor α (TNF- α) were detected in response to repeated stimulation by heat-inactivated *E. coli*. All CPEM samples, except those stimulated with smooth hydroxyapatite particles of ~100 μm in size, exhibited reduced interleukin 10 (IL-10) production. All this, coupled with the dynamics of mast cell and

resident macrophage infiltration, indicates a less significant inflammatory response for large spherical particles compared to needle particles [224]. Moreover, the authors of some studies draw conclusions about the extremely high importance of transplant morphology for the formation of osteoconductive properties, focusing on the rate of material resorption by TRAP-positive osteoclast-like cells and TRAP-negative multinucleated giant cells [225].

Comparatively more recent studies also confirm the special importance of the nano-level morphology of hydroxyapatite-based grafting material. Artificially engineered microgrooved hydroxyapatite surface structure promotes macrophage attachment and reduced synthesis of pro-inflammatory cytokines TNF- α , IL-1 β and interleukin 6 (IL-6) compared to standard porous hydroxyapatite framework by reducing the accumulation of reactive oxygen species through modulation of mitochondrial functions. However, no effect on the nature and dynamics of macrophage polarization was found [226], although more recent studies report such a possibility [5].

On the other hand, upon exposure to nanostructured hydroxyapatite, a marked increase in the secretion of TNF- α and IL-6, as well as adenosine triphosphate, nicotinamideadenine dinucleotide and reactive oxygen species [227], interferon γ (IFN- γ) and cluster of differentiation 107 α (CD107 α) on cluster of differentiation 8 (CD8)-positive T cells [228] were observed in macrophages, against a background of decreased IL-10 production. In contrast, the microgroove structure promoted the viability of bone marrow mesenchymal stem cells by inhibiting miR-214 by reducing IL-6 [226]. Also, the ability of rod-shaped hydroxyapatite to exert a marked effect on mitochondrial functionality is confirmed by its use as an effective antitumor agent. Hydroxyapatite with the above morphology has notable immunomodulatory [220,229] and proapoptotic properties [220], as the release of cathepsin B and generation of mitochondrial reactive oxygen species are observed upon internalization of nanorod hydroxyapatite [228].

The following literature example is key, as this work particularly demonstrates the difference between the effects of hydroxyapatite morphology under in vivo and in vitro conditions: in the former, we observe a distinctly higher osteoconductive potential of nanostructured hydroxyapatite and a smaller osteoclast area compared to submicron-sized hydroxyapatite; in the second case, despite the highest cell viability rate at the earliest stages of co-culture for the nanostructured hydroxyapatite, a more mature osteoclast morphology and significantly higher expression of osteoclast-associated genes over a medium time distance were detected for the submicron form of hydroxyapatite [205].

Taking into account all the data presented above, including data on ribosomal [217] and mitochondrial [220] mechanism of inhibition of cell development, as well as the ability of nanostructured hydroxyapatite to activate osteoclasts [222], the most important parameter in the response to morphological characterization of the material is a relatively constant and prolonged infiltration of immune cells. This is achievable only in living conditions, which can be indirectly confirmed by the dynamics of infiltration of resident macrophages and mast cells for the small-sized form of hydroxyapatite [224].

6. Conclusion and Future Directions

From the very beginning of this analytical review, a hypothetical possibility of a special character of the relationship between the mineral component of bone tissue and mitochondria was presented. It is quite possible that the direct beginning of bone tissue mineralization is provided by energy-dependent movement of Ca²⁺ cations and serum phosphate ions into mitochondria of osteoblasts and subsequent deposition of amorphous calcium phosphate micropackages. At the same time, the extremely important role of mitochondria in the metabolism of both synthetic hydroxyapatite in the form of bone grafting material and native bone tissue hydroxyapatite has been proven. On the other hand, the effect of hydroxyapatite on mitochondrial function in the role of key regulators of calcium homeostasis of the cell is extremely appreciated. The semantic coherence of the presented data may indicate the necessity to analyze various disorders of bone tissue mineral component metabolism from the point of view in which mitochondria of osteoblasts, osteocytes and, especially, osteoclasts serve as the key apparatus for its formation.

Also, as a result of this work, numerous literature data have been cited, which form a fairly complete picture of the differences between the results of in vivo and in vitro studies of synthetic hydroxyapatite with a variety of nanoscale morphologies. First of all, we conclude that an adequate evaluation of hydroxyapatite as a grafting material with nano-sized morphology at this stage is possible only under relatively constant and prolonged infiltration of immune cells under the condition of sufficient duration of analysis. These conditions can only be fully achieved by using in vivo studies.

In addition, the key features of hydroxyapatite as a bone grafting material, which include a special character of interaction with monocytes/macrophages, osteoclasts and T-cells of the recipient's body. Moreover, this property can be directly regulated by the nanoscale morphology of the material, provided that its macroscopic structure is preserved. Recently, the ability of hydroxyapatite nanoparticles to influence ribosomes and mitochondria of many cells is of particular interest. Together with satisfactory mechanical properties, high potential for scalability and unification of the production process, this material is the most suitable for the treatment of extensive bone defects of tumor origin.

Thus, this work highlights a potential and relatively original theoretical direction for future research on hydroxyapatite in the role of bone grafting material. We also demonstrate the relatively high value of the results of in vivo studies, which in itself is not original. However, it justifies the need to intensify the development of in vitro research methods towards biomimetic studies.

Author Contributions: Conceptualization, M.C. and A.V.S.; methodology, M.C. and A.V.S.; formal analysis, E.S. and G.S.; investigation, M.C. and A.V.S.; resources, M.C., A.V.S. and E.S.; writing—original draft preparation, M.C. and A.V.S.; writing—review and editing, E.S., G.S. and C.C.R.; visualization, E.S. and C.C.R.; supervision, E.S. All authors have read and agreed to the published version of the manuscript.

Funding: This study was supported by the Russian Science Foundation under grant № 23-15-20042.

Institutional Review Board Statement: Not applicable.

Informed Consent Statement: Not applicable.

Data Availability Statement: Not applicable.

Conflicts of Interest: The authors declare no conflict of interest

References

1. Luedemann R.E., Thomas K.A., Cook S.D. Particulate aluminum oxide as a bone graft material. *Biomater Med Devices Artif Organs* 1986; 14(3-4):257-73. <https://doi.org/10.3109/10731198609117547>.
2. Kim J.M., Son J.S., Kang S.S., Kim G., Choi S.H. Bone regeneration of hydroxyapatite/alumina bilayered scaffold with 3 mm passage-like medullary canal in canine tibia model. *Biomed Res Int* 2015; 2015:235108. <https://doi.org/10.1155/2015/235108>.
3. Pujari S., Hoess A., Shen J., Thormann A., Heilmann A., Tang L., Karlsson-Ott M. Effects of nanoporous alumina on inflammatory cell response. *J Biomed Mater Res A* 2014; 102(11):3773-80. <https://doi.org/10.1002/jbm.a.35048>.
4. Mahon O.R., Browe D.C., Gonzalez-Fernandez T., Pitacco P., Whelan I.T., Von Euw S., Hobbs C., Nicolosi V., Cunningham K.T., Mills K.H.G., Kelly D.J., Dunne A. Nano-particle mediated M2 macrophage polarization enhances bone formation and MSC osteogenesis in an IL-10 dependent manner. *Biomaterials* 2020; 239:119833. <https://doi.org/10.1016/j.biomaterials.2020.119833>.
5. Wang R., Hua Y., Wu H., Wang J., Xiao Y.C., Chen X., Ao Q., Zeng Q., Zhu X., Zhang X. Hydroxyapatite nanoparticles promote TLR4 agonist-mediated anti-tumor immunity through synergically enhanced macrophage polarization. *Acta Biomater* 2023; 164:626-640. <https://doi.org/10.1016/j.actbio.2023.04.027>.
6. Burr D.B. Changes in bone matrix properties with aging. *Bone* 2019; 120:85-93. <https://doi.org/10.1016/j.bone.2018.10.010>.
7. Sobczak-Kupiec A., Drabczyk A., Florkiewicz W., Głab M., Kudłacik-Kramarczyk S., Słota D., Tomala A., Tyliczszak B. Review of the Applications of Biomedical Compositions Containing Hydroxyapatite and Collagen Modified by Bioactive Components. *Materials (Basel)* 2021; 14(9):2096. <https://doi.org/10.3390/ma14092096>.
8. Veremeiev A., Bolgarin R., Nesterenko V., Andreev-Andrievskiy A., Kutikhin A. Native Bovine Hydroxyapatite Powder, Demineralised Bone Matrix Powder, and Purified Bone Collagen Membranes Are

- Efficient in Repair of Critical-Sized Rat Calvarial Defects. *Materials* (Basel) 2020; 13(15):3393. <https://doi.org/10.3390/ma13153393>.
9. Indurkar A., Choudhary R., Rubenis K., Locs J. Role of carboxylic organic molecules in interfibrillar collagen mineralization. *Front Bioeng Biotechnol* 2023; 11:1150037. <https://doi.org/10.3389/fbioe.2023.1150037>.
 10. Simon P., Grüner D., Worch H., Pompe W., Lichte H., El Khassawna T., Heiss C., Wenisch S., Kniep R. First evidence of octacalcium phosphate@osteocalcin nanocomplex as skeletal bone component directing collagen triple-helix nanofibril mineralization. *Sci Rep* 2018; 8(1):13696. <https://doi.org/10.1038/s41598-018-31983-5>.
 11. Carvalho M.S., Cabral J.M.S., da Silva C.L., Vashishth D. Bone Matrix Non-Collagenous Proteins in Tissue Engineering: Creating New Bone by Mimicking the Extracellular Matrix. *Polymers* (Basel) 2021; 13(7):1095. <https://doi.org/10.3390/polym13071095>.
 12. Xu Z., Yang C., Wu F., Tan X., Guo Y., Zhang H., Wang H., Sui X., Xu Z., Zhao M., Jiang S., Dai Z., Li Y. Triple-gene deletion for osteocalcin significantly impairs the alignment of hydroxyapatite crystals and collagen in mice. *Front Physiol.* 2023 Mar 28; 14:1136561. <https://doi.org/10.3389/fphys.2023.1136561>.
 13. Koblenzer M., Weiler M., Fragoulis A., Rütten S., Pufe T., Jahr H. Physiological Mineralization during In Vitro Osteogenesis in a Biomimetic Spheroid Culture Model. *Cells* 2022; 11(17):2702. <https://doi.org/10.3390/cells11172702>.
 14. Pastero L., Bruno M., Aquilano D. Habit Change of Monoclinic Hydroxyapatite Crystals Growing from Aqueous Solution in the Presence of Citrate Ions: The Role of 2D Epitaxy. *Crystals* 2018; 8(8). 308. <https://doi.org/10.3390/cryst8080308>
 15. Nudelman F., Pieterse K., George A., Bomans P.H., Friedrich H., Brylka L.J., Hilbers P.A., de With G., Sommerdijk N.A. The role of collagen in bone apatite formation in the presence of hydroxyapatite nucleation inhibitors. *Nat Mater* 2010; 9(12):1004-9. <https://doi.org/10.1038/nmat2875>.
 16. Kawska A., Hochrein O., Brickmann J., Kniep R., Zahn D. The nucleation mechanism of fluorapatite-collagen composites: ion association and motif control by collagen proteins. *Angew Chem Int Ed Engl* 2008; 47(27):4982-5. <https://doi.org/10.1002/anie.200800908>.
 17. Moriishi T., Ozasa R., Ishimoto T., Nakano T., Hasegawa T., Miyazaki T., Liu W., Fukuyama R., Wang Y., Komori H., Qin X., Amizuka N., Komori T. Osteocalcin is necessary for the alignment of apatite crystallites, but not glucose metabolism, testosterone synthesis, or muscle mass. *PLoS Genet* 2020; 16(5):e1008586. <https://doi.org/10.1371/journal.pgen.1008586>.
 18. Komori T. What is the function of osteocalcin? *J Oral Biosci* 2020; 62(3):223-227. <https://doi.org/10.1016/j.job.2020.05.004>.
 19. Wang B., Zhang Z., Pan H. Bone Apatite Nanocrystal: Crystalline Structure, Chemical Composition, and Architecture. *Biomimetics* (Basel) 2023; 8(1):90. <https://doi.org/10.3390/biomimetics8010090>.
 20. Fleet M.E. The carbonate ion in hydroxyapatite: recent X-ray and infrared results. *Front Biosci (Elite Ed)* 2013; 5(2):643-52. <https://doi.org/10.2741/e645>.
 21. Bonar L.C., Shimizu M., Roberts J.E., Griffin R.G., Glimcher M.J. Structural and composition studies on the mineral of newly formed dental enamel: a chemical, x-ray diffraction, and ³¹P and proton nuclear magnetic resonance study. *J Bone Miner Res* 1991; 6(11):1167-76. <https://doi.org/10.1002/jbmr.5650061105>.
 22. Bang L.T., Long B.D., Othman R. Carbonate hydroxyapatite and silicon-substituted carbonate hydroxyapatite: synthesis, mechanical properties, and solubility evaluations. *ScientificWorldJournal* 2014; 2014:969876. <https://doi.org/10.1155/2014/969876>.
 23. Saghir M.A., Vakhnovetsky J., Vakhnovetsky A., Ghobrial M., Nath D., Morgano S.M. Functional role of inorganic trace elements in dentin apatite tissue-Part 1: Mg, Sr, Zn, and Fe. *J Trace Elem Med Biol* 2022; 71:126932. <https://doi.org/10.1016/j.jtemb.2022.126932>.
 24. Landis W.J., Glimcher M.J. Electron diffraction and electron probe microanalysis of the mineral phase of bone tissue prepared by anhydrous techniques. *J Ultrastruct Res* 1978; 63(2):188-223. [https://doi.org/10.1016/s0022-5320\(78\)80074-4](https://doi.org/10.1016/s0022-5320(78)80074-4).
 25. Bigi A., Boanini E., Gazzano M. Ion Substitution in Biological and Synthetic Apatites. 2016. 235-266. <https://doi.org/10.1016/B978-1-78242-338-6.00008-9>
 26. Bertinetti L., Tampieri A., Landi E., Ducati C., Midgley P. A., Coluccia S., Martra G. Surface structure, hydration, and cationic sites of nanohydroxyapatite: UHR-TEM, IR, and microgravimetric studies. *Journal of Physical Chemistry C* 2007; 111(10): 4027–4035. <https://doi.org/10.1021/jp066040s>
 27. Bres E.F., Steuer P., Voegel J.C., Frank R.M., Cuisinier F.J. Observation of the loss of the hydroxyapatite sixfold symmetry in a human fetal tooth enamel crystal. *J Microsc* 1993; 170(Pt 2):147-54. <https://doi.org/10.1111/j.1365-2818.1993.tb03334.x>.
 28. LeGeros R.Z., Ito A., Ishikawa K., Sakae T., LeGeros J.P. Fundamentals of hydroxyapatite and related calcium phosphates. *Adv. Biomater. Fundam. Process. Appl.* 2009; 19–52. <https://doi.org/10.1002/9780470891315.ch2>

29. Rey C., Renugopalakrishnan V., Collins B., Glimcher M.J. Fourier transform infrared spectroscopic study of the carbonate ions in bone mineral during aging. *Calcif Tissue Int* 1991; 49(4):251-8. <https://doi.org/10.1007/BF02556214>.
30. Suzuki O., Hamai R., Sakai S. The material design of octacalcium phosphate bone substitute: increased dissolution and osteogenicity. *Acta Biomater* 2023; 158:1-11. <https://doi.org/10.1016/j.actbio.2022.12.046>.
31. Zhou C., Zhang X., Ai J. et al. Chiral hierarchical structure of bone minerals. *Nano Res* 2022; 15:1295–1302. <https://doi.org/10.1007/s12274-021-3653-z>
32. Guarino V., Veronesi F., Marrese M., Giavaresi G., Ronca A., Sandri M., Tampieri A., Fini M., Ambrosio L. Needle-like ion-doped hydroxyapatite crystals influence osteogenic properties of PCL composite scaffolds. *Biomed Mater* 2016; 11(1):015018. <https://doi.org/10.1088/1748-6041/11/1/015018>.
33. Yamamoto T., Hasegawa T., Hongo H., Amizuka N. Alternating lamellar structure in human cellular cementum and rat compact bone: Its structure and formation. *J Oral Biosci* 2019; 61(2):105-114. <https://doi.org/10.1016/j.job.2019.03.006>.
34. Pazzaglia U.E., Congiu T., Marchese M., Spagnuolo F., Quacci D. Morphometry and patterns of lamellar bone in human Haversian systems. *Anat Rec (Hoboken)* 2012; 295(9):1421-9. doi: 10.1002/ar.22535.
35. Locke M. Structure of long bones in mammals. *J Morphol* 2004; 262(2):546-65. <https://doi.org/10.1002/jmor.10282>.
36. Schmidt A.H. Autologous bone graft: Is it still the gold standard? *Injury*. 2021; 52 Suppl 2:S18-S22. <https://doi.org/10.1016/j.injury.2021.01.043>.
37. Dissaux C., Ruffenach L., Bruant-Rodier C., George D., Bodin F., Rémond Y. Cleft Alveolar Bone Graft Materials: Literature Review. *Cleft Palate Craniofac J* 2022; 59(3):336-346. <https://doi.org/10.1177/10556656211007692>.
38. Giannoudis P.V., Einhorn T.A., Marsh D. Fracture healing: The diamond concept. *Injury* 2007; 38: S3-S6. [https://doi.org/10.1016/S0020-1383\(08\)70003-2](https://doi.org/10.1016/S0020-1383(08)70003-2).
39. Kamal M., Gremse F., Rosenhain S., Bartella A.K., Hölzle F., Kessler P., Lethaus B. Comparison of Bone Grafts From Various Donor Sites in Human Bone Specimens. *J Craniofac Surg* 2018; 29(6):1661-1665. <https://doi.org/10.1097/SCS.0000000000004586>.
40. Hamada T., Matsubara H., Hikichi T., Shimokawa K., Tsuchiya H. Rat model of an autologous cancellous bone graft. *Sci Rep* 2021; 11(1):18001. <https://doi.org/10.1038/s41598-021-97573-0>.
41. Mehta D.D., Dankert J.F., Buchalter D.B., Kirby D.J., Patel K.S., Rocks M., Hacquebord J.H., Leucht P. Iliac Crest and Distal Radius Autografts Exhibit Distinct Cell-Intrinsic Functional Differences. *J Hand Surg Am* 2022; S0363-5023(22)00330-6. <https://doi.org/10.1016/j.jhsa.2022.06.005>.
42. Stahl A., Yang Y.P. Regenerative Approaches for the Treatment of Large Bone Defects. *Tissue Eng Part B Rev* 2021; 27(6):539-547. <https://doi.org/10.1089/ten.TEB.2020.0281>.
43. Taqi M., Llewellyn C.M., Estefan M. Fibula Tissue Transfer 2023; In: StatPearls [Internet]. Treasure Island (FL): StatPearls Publishing. <https://www.ncbi.nlm.nih.gov/books/NBK563283/>
44. Fillingham Y., Jacobs J. Bone grafts and their substitutes. *Bone Joint J.* 2016; 98-B(1 Suppl A):6-9. <https://doi.org/10.1302/0301-620X.98B.36350>.
45. Street M., Gao R., Martis W., Munro J., Musson D., Cornish J., Ferguson J. The Efficacy of Local Autologous Bone Dust: A Systematic Review. *Spine Deform* 2017; 5(4):231-237. <https://doi.org/10.1016/j.jspsd.2017.02.003>.
46. Hazbulla D., Inchingolo A.D., Inchingolo A.M., Malcangi G., Santacroce L., Minetti E., Di Venere D., Limongelli L., Bordea I.R., Scarano A., Lorusso F., Xhajanka E., Laforgia A., Inchingolo F., Greco Lucchina A., Dipalma G. The effectiveness of autologous demineralized tooth graft for the bone ridge preservation: a systematic review of the literature. *J Biol Regul Homeost Agents* 2021; 35(2 Suppl. 1):283-294. <https://doi.org/10.23812/21-2suppl1-28>.
47. Peterson J.R., Chen F., Nwankwo E., Dekker T.J., Adams S.B. The Use of Bone Grafts, Bone Graft Substitutes, and Orthobiologics for Osseous Healing in Foot and Ankle Surgery. *Foot Ankle Orthop* 2019; 4(3):2473011419849019. <https://doi.org/10.1177/2473011419849019>.
48. Al-Moraissi E.A., Alkhutari A.S., Abotaleb B., Altairi N.H., Del Fabbro M. Do osteoconductive bone substitutes result in similar bone regeneration for maxillary sinus augmentation when compared to osteogenic and osteoinductive bone grafts? A systematic review and frequentist network meta-analysis. *Int J Oral Maxillofac Surg* 2020; 49(1):107-120. <https://doi.org/10.1016/j.ijom.2019.05.004>.
49. Green J. History and development of suction-irrigation-reaming. *Injury* 2010; 41 Suppl 2:S24-31. [https://doi.org/10.1016/S0020-1383\(10\)70005-X](https://doi.org/10.1016/S0020-1383(10)70005-X).
50. van de Wall B.J.M., Beeres F.J.P., Rompen I.F., Link B.C., Babst R., Schoeneberg C., Michelitsch C., Nebelung S., Pape H.C., Gueorguiev B., Knobe M. RIA versus iliac crest bone graft harvesting: A meta-analysis and systematic review. *Injury* 2022; 53(2):286-293. <https://doi.org/10.1016/j.injury.2021.10.002>.
51. Laubach M., Weimer L.P., Bläsius F.M., Hildebrand F., Kobbe P., Hutmacher D.W. Complications associated using the reamer-irrigator-aspirator (RIA) system: a systematic review and meta-analysis. *Arch Orthop Trauma Surg* 2023; 143(7):3823-3843. <https://doi.org/10.1007/s00402-022-04621-z>.

52. Chen N.T., Glowacki J., Bucky L.P., Hong H.Z., Kim W.K., Yaremchuk M.J. The roles of revascularization and resorption on endurance of craniofacial onlay bone grafts in the rabbit. *Plast Reconstr Surg* 1994; 93(4):714-22; discussion 723-4.
53. Burchardt H. The biology of bone graft repair. *Clin Orthop Relat Res*. 1983; (174):28-42.
54. Ku J.K., Ghim M.S., Park J.H., Leem D.H. A ramus cortical bone harvesting technique without bone marrow invasion. *J Korean Assoc Oral Maxillofac Surg* 2023; 49(2):100-104. <https://doi.org/10.5125/jkaoms.2023.49.2.100>.
55. Vandeputte T., Bigorre M., Tramini P., Captier G. Comparison between combined cortical and cancellous bone graft and cancellous bone graft in alveolar cleft: Retrospective study of complications during the first six months post-surgery. *J Craniomaxillofac Surg* 2020; 48(1):38-42. <https://doi.org/10.1016/j.jcms.2019.11.013>.
56. Ogden N.K.E., Jukic C.C., Zedler S.T. Management of an extensive equine juvenile ossifying fibroma by rostral mandibulectomy and reconstruction of the mandibular symphysis using String of Pearls plates with cortical and cancellous bone autografts. *Vet Surg* 2019; 48(1):105-111. <https://doi.org/10.1111/vsu.12943>.
57. Kobbe P., Laubach M., Hutmacher D.W., Alabdulrahman H., Sellei R.M., Hildebrand F. Convergence of scaffold-guided bone regeneration and RIA bone grafting for the treatment of a critical-sized bone defect of the femoral shaft. *Eur J Med Res* 2020; 25(1):70. <https://doi.org/10.1186/s40001-020-00471-w>.
58. Ehredt D.J. Jr., Rogers B., Takhar J., Payton P., Siesel K. Percutaneous Harvest of Calcaneal Bone Autograft: Quantification of Volume and Definition of Anatomical Safe Zone. *J Foot Ankle Surg* 2022 Jan; 61(1):27-31. <https://doi.org/10.1053/j.jfas.2021.06.001>.
59. Dimitriou R., Mataliotakis G.I., Angoules A.G., Kanakaris N.K., Giannoudis P.V. Complications following autologous bone graft harvesting from the iliac crest and using the RIA: a systematic review. *Injury* 2011; 42 Suppl 2:S3-15. <https://doi.org/10.1016/j.injury.2011.06.015>.
60. Suda A.J., Schamberger C.T., Viergutz T. Donor site complications following anterior iliac crest bone graft for treatment of distal radius fractures. *Arch Orthop Trauma Surg* 2019; 139(3):423-428. <https://doi.org/10.1007/s00402-018-3098-3>.
61. Li G., Li P., Chen Q., Thu H.E., Hussain Z. Current Updates on Bone Grafting Biomaterials and Recombinant Human Growth Factors Implanted Biotherapy for Spinal Fusion: A Review of Human Clinical Studies. *Curr Drug Deliv* 2019; 16(2):94-110. <https://doi.org/10.2174/1567201815666181024142354>.
62. Smeets R., Matthies L., Windisch P., Gosau M., Jung R., Brodala N., Stefanini M., Kleinheinz J., Payer M., Henningsen A., Al-Nawas B., Knipfer C. Horizontal augmentation techniques in the mandible: a systematic review. *Int J Implant Dent* 2022; 8(1):23. <https://doi.org/10.1186/s40729-022-00421-7>.
63. Sharifi M., Kheradmandi R., Salehi M., Alizadeh M., Ten Hagen T.L.M., Falahati M. Criteria, Challenges, and Opportunities for Acellularized Allogeneic/Xenogeneic Bone Grafts in Bone Repairing. *ACS Biomater Sci Eng* 2022; 8(8):3199-3219. <https://doi.org/10.1021/acsbiomaterials.2c00194>.
64. Salem D., Alshihri A., Arguello E., Jung R.E., Mohamed H.A., Friedland B. Volumetric Analysis of Allogenic and Xenogenic Bone Substitutes Used in Maxillary Sinus Augmentations Utilizing Cone Beam CT: A Prospective Randomized Pilot Study. *Int J Oral Maxillofac Implants* 2019; 34(4):920-926. <https://doi.org/10.11607/jomi.7318>.
65. Govoni M., Vivarelli L., Mazzotta A., Stagni C., Maso A., Dallari D. Commercial Bone Grafts Claimed as an Alternative to Autografts: Current Trends for Clinical Applications in Orthopaedics. *Materials (Basel)* 2021; 14(12):3290. <https://doi.org/10.3390/ma14123290>.
66. Jordana F., Le Visage C., Weiss P. Substituts osseux [Bone substitutes]. *Med Sci (Paris)* 2017; 33(1):60-65. French. <https://doi.org/10.1051/medsci/20173301010>.
67. Lomas R., Chandrasekar A., Board T.N. Bone allograft in the U.K.: perceptions and realities. *Hip Int* 2013; 23(5):427-33. <https://doi.org/10.5301/hipint.5000018>.
68. Scheufler K.M., Diesing D. Einsatz von Knochenersatzmaterialien bei Fusionen der Wirbelsäule [Use of bone graft replacement in spinal fusions]. *Orthopade* 2015; 44(2):146-53. German. <https://doi.org/10.1007/s00132-014-3069-5>.
69. Brink O. The choice between allograft or demineralized bone matrix is not unambiguous in trauma surgery. *Injury* 2021; 52 Suppl 2:S23-S28. <https://doi.org/10.1016/j.injury.2020.11.013>.
70. Windhager R., Hobusch G.M., Matzner M. Allogene Transplantate für biologische Rekonstruktionen von Knochendefekten [Allogeneic transplants for biological reconstruction of bone defects]. *Orthopade* 2017; 46(8):656-664. German. <https://doi.org/10.1007/s00132-017-3452-0>.
71. Eppey B.L., Pietrzak W.S., Blanton M.W. Allograft and alloplastic bone substitutes: a review of science and technology for the craniomaxillofacial surgeon. *J Craniofac Surg* 2005; 16(6):981-9. <https://doi.org/10.1097/01.scs.0000179662.38172.dd>.
72. Kotelnikov G.P., Kolsanov A.V., Volova L.T., Trunin D.A., Popov N.V., Nikolaenko A.N., Stepanov G.V. Tekhnologiya proizvodstva personalizirovannogo rekonstruktivnogo allogennogo kostnogo implantata [Technology of manufacturing of personalized reconstructive allogenic bone graft (in Russian only)]. *Khirurgiya (Mosk)* 2019; (3):65-72. Russian. <https://doi.org/10.17116/hirurgia201903165>.

73. Weinraub G.M. Orthobiologics: a survey of materials and techniques. *Clin Podiatr Med Surg* 2005; 22(4):509-19, v. <https://doi.org/10.1016/j.cpm.2005.08.003>.
74. Gruskin E., Doll B.A., Futrell F.W., Schmitz J.P., Hollinger J.O. Demineralized bone matrix in bone repair: history and use. *Adv Drug Deliv Rev* 2012; 64(12):1063-77. <https://doi.org/10.1016/j.addr.2012.06.008>.
75. Dinopoulos H.T., Giannoudis P.V. Safety and efficacy of use of demineralised bone matrix in orthopaedic and trauma surgery. *Expert Opin Drug Saf* 2006; 5(6):847-66. <https://doi.org/10.1517/14740338.5.6.847>.
76. Wu J., Liu F., Wang Z., Liu Y., Zhao X., Fang C., Leung F., Yeung K.W.K., Wong T.M. The Development of a Magnesium-Releasing and Long-Term Mechanically Stable Calcium Phosphate Bone Cement Possessing Osteogenic and Immunomodulation Effects for Promoting Bone Fracture Regeneration. *Front Bioeng Biotechnol* 2022; 9:803723. <https://doi.org/10.3389/fbioe.2021.803723>.
77. Würdinger R., Donkiewicz P. Allogeneic cortical struts and bone granules for challenging alveolar reconstructions: An innovative approach toward an established technique. *J Esthet Restor Dent* 2020; 32(8):747-756. <https://doi.org/10.1111/jerd.12639>.
78. Bieganowski T., Buchalter D.B., Singh V., Mercuri J.J., Aggarwal V.K., Rozell J.C., Schwarzkopf R. Bone loss in aseptic revision total knee arthroplasty: management and outcomes. *Knee Surg Relat Res* 2022; 34(1):30. <https://doi.org/10.1186/s43019-022-00158-y>.
79. Wildemann B., Kadow-Romacker A., Pruss A., Haas N.P., Schmidmaier G. Quantification of growth factors in allogenic bone grafts extracted with three different methods. *Cell Tissue Bank* 2007; 8(2):107-14. <https://doi.org/10.1007/s10561-006-9021-0>.
80. Blokhuis T.J., Arts J.J. Bioactive and osteoinductive bone graft substitutes: definitions, facts and myths. *Injury* 2011; 42 Suppl 2:S26-9. <https://doi.org/10.1016/j.injury.2011.06.010>.
81. Rocha T., Cavalcanti A.S., Leal A.C., Dias R.B., da Costa R.S., Ribeiro G.O., Guimarães J.A.M., Duarte M.E.L. PTH₁₋₃₄ improves devitalized allogenic bone graft healing in a murine femoral critical size defect. *Injury* 2021; 52 Suppl 3:S3-S12. <https://doi.org/10.1016/j.injury.2021.03.063>.
82. Golubovsky J.L., Ejikeme T., Winkelman R., Steinmetz M.P. Osteobiologics. *Oper Neurosurg (Hagerstown)* 2021; 21(Suppl 1):S2-S9. <https://doi.org/10.1093/ons/opaa383>.
83. Veronesi F., Martini L., Giavaresi G., Fini M. Bone regenerative medicine: metatarsus defects in sheep to evaluate new therapeutic strategies for human long bone defect. A systematic review. *Injury* 2020; 51(7):1457-1467. <https://doi.org/10.1016/j.injury.2020.04.010>.
84. Shih S., Askinas C., Caughey S., Vernice N., Berri N., Dong X., Spector J.A. Sourcing and development of tissue for transplantation in reconstructive surgery: A narrative review. *J Plast Reconstr Aesthet Surg* 2023; 83:266-275. <https://doi.org/10.1016/j.bjps.2023.05.001>.
85. Płomiński J., Kwiatkowski K. Przeszczepy kostne [Bone grafts (editorial)]. *Pol Merkur Lekarski* 2006; 21(126):507-10. Polish.
86. Kwiecien G.J., Aliotta R., Bassiri Gharb B., Gastman B., Zins J.E. The Timing of Alloplastic Cranioplasty in the Setting of Previous Osteomyelitis. *Plast Reconstr Surg* 2019; 143(3):853-861. <https://doi.org/10.1097/PRS.0000000000005363>.
87. Egol K.A., Nauth A., Lee M., Pape H.C., Watson J.T., Borrelli J. Jr. Bone Grafting: Sourcing, Timing, Strategies, and Alternatives. *J Orthop Trauma* 2015; 29 Suppl 12:S10-4. <https://doi.org/10.1097/BOT.0000000000000460>.
88. Viola A. 3rd, Appiah J., Donnally C.J. 3rd, Kim Y.H., Shenoy K. Bone Graft Options in Spinal Fusion: A Review of Current Options and the Use of Mesenchymal Cellular Bone Matrices. *World Neurosurg* 2022; 158:182-188. <https://doi.org/10.1016/j.wneu.2021.11.130>.
89. Abedi A., Formanek B., Russell N., Vizesi F., Boden S.D., Wang J.C., Buser Z. Examination of the Role of Cells in Commercially Available Cellular Allografts in Spine Fusion: An in Vivo Animal Study. *J Bone Joint Surg Am* 2020; 102(24):e135. <https://doi.org/10.2106/JBJS.20.00330>.
90. Kinaia B.M., Daweri O., Gala R., Turows A., Harunani A., Neely A.L. Management of vertical bony defect using novel xenogeneic/allogeneic bone graft: A case report. *Clin Adv Periodontics* 2023. <https://doi.org/10.1002/cap.10256>.
91. Bansal M.R., Bhagat S.B., Shukla D.D. Bovine cancellous xenograft in the treatment of tibial plateau fractures in elderly patients. *Int Orthop* 2009; 33(3):779-84. <https://doi.org/10.1007/s00264-008-0526-y>.
92. Naros A., Bayazeed B., Schwarz U., Nagursky H., Reinert S., Schmelzeisen R., Sauerbier S. A prospective histomorphometric and cephalometric comparison of bovine bone substitute and autogenous bone grafting in Le Fort I osteotomies. *J Craniomaxillofac Surg* 2019; 47(2):233-238. <https://doi.org/10.1016/j.jcms.2018.11.032>.
93. Lim J., Jun S.H., Tallarico M., Park J.B., Park D.H., Hwang K.G., Park C.J. A Randomized Controlled Trial of Guided Bone Regeneration for Peri-Implant Dehiscence Defects with Two Anorganic Bovine Bone Materials Covered by Titanium Meshes. *Materials (Basel)* 2022; 15(15):5294. <https://doi.org/10.3390/ma15155294>.
94. Tawil G., Barbeck M., Unger R., Tawil P., Witte F. Sinus Floor Elevation Using the Lateral Approach and Window Repositioning and a Xenogeneic Bone Substitute as a Grafting Material: A Histologic,

- Histomorphometric, and Radiographic Analysis. *Int J Oral Maxillofac Implants* 2018; 33(5):1089–1096. <https://doi.org/10.11607/jomi.6226>.
95. Ding Y., Wang L., Su K., Gao J., Li X., Cheng G. Horizontal bone augmentation and simultaneous implant placement using xenogeneic bone rings technique: a retrospective clinical study. *Sci Rep* 2021; 11(1):4947. <https://doi.org/10.1038/s41598-021-84401-8>.
 96. Shibuya N., Holloway B.K., Jupiter D.C. A comparative study of incorporation rates between non-xenograft and bovine-based structural bone graft in foot and ankle surgery. *J Foot Ankle Surg* 2014; 53(2):164-7. <https://doi.org/10.1053/j.jfas.2013.10.013>.
 97. Shibuya N., Jupiter D.C. Bone graft substitute: allograft and xenograft. *Clin Podiatr Med Surg* 2015; 32(1):21-34. <https://doi.org/10.1016/j.cpm.2014.09.011>.
 98. Schwarz F., Ferrari D., Balic E., Buser D., Becker J., Sager M. Lateral ridge augmentation using equine- and bovine-derived cancellous bone blocks: a feasibility study in dogs. *Clin Oral Implants Res* 2010; 21(9):904-12. <https://doi.org/10.1111/j.1600-0501.2010.01951.x>.
 99. Ledford C.K., Nunley J.A. 2nd, Viens N.A., Lark R.K. Bovine xenograft failures in pediatric foot reconstructive surgery. *J Pediatr Orthop* 2013; 33(4):458-63. <https://doi.org/10.1097/BPO.0b013e318287010d>.
 100. Balduw P., Li D.J., Auston D.A., Mir H.S., Yoon R.S., Koval K.J. Autograft, Allograft, and Bone Graft Substitutes: Clinical Evidence and Indications for Use in the Setting of Orthopaedic Trauma Surgery. *J Orthop Trauma* 2019; 33(4):203-213. <https://doi.org/10.1097/BOT.0000000000001420>.
 101. Ruffilli A., Barile F., Fiore M., Manzetti M., Viroli G., Mazzotti A., Govoni M., De Franceschi L., Dallari D., Faldini C. Allogenic bone grafts and postoperative surgical site infection: are positive intraoperative swab cultures predictive for a higher infectious risk? *Cell Tissue Bank* 2023; 24(3):627-637. <https://doi.org/10.1007/s10561-022-10061-1>.
 102. Singh S., Verma A., Jain A., Goyal T., Kandwal P., Arora S.S. Infection and utilization rates of bone allografts in a hospital-based musculoskeletal tissue bank in north India. *J Clin Orthop Trauma* 2021; 23:101635. <https://doi.org/10.1016/j.jcot.2021.101635>.
 103. Van Der Merwe W., Lind M., Faunø P., Van Egmond K., Zaffagnini S., Marcacci M., Cugat R., Verdonk R., Ibañez E., Guillen P., Marcheggiani Muccioli G.M. Xenograft for anterior cruciate ligament reconstruction was associated with high graft processing infection. *J Exp Orthop* 2020; 7(1):79. <https://doi.org/10.1186/s40634-020-00292-0>.
 104. Graham S.M., Leonidou A., Aslam-Pervez N., Hamza A., Panteliadis P., Heliotis M., Mantalaris A., Tsiroidis E. Biological therapy of bone defects: the immunology of bone allo-transplantation. *Expert Opin Biol Ther* 2010; 10(6):885-901. <https://doi.org/10.1517/14712598.2010.481669>.
 105. Hinsenkamp M., Muylle L., Eastlund T., Fehily D., Noël L., Strong D.M. Adverse reactions and events related to musculoskeletal allografts: reviewed by the World Health Organisation Project NOTIFY. *Int Orthop* 2012; 36(3):633-41. <https://doi.org/10.1007/s00264-011-1391-7>.
 106. Wei L., Ma B.J., Shao J.L., Ge S.H. [Advances in the Application of Hydroxyapatite Composite Materials in Bone Tissue Engineering]. *Sichuan Da Xue Xue Bao Yi Xue Ban* 2021; 52(3):357-363. Chinese. <https://doi.org/10.12182/20210560303>.
 107. George S.M., Nayak C., Singh I., Balani K. Multifunctional Hydroxyapatite Composites for Orthopedic Applications: A Review. *ACS Biomater Sci Eng* 2022; 8(8):3162-3186. <https://doi.org/10.1021/acsbiomaterials.2c00140>.
 108. Zaed I., Cardia A., Stefini R. From Reparative Surgery to Regenerative Surgery: State of the Art of Porous Hydroxyapatite in Cranioplasty. *Int J Mol Sci* 2022; 23(10):5434. <https://doi.org/10.3390/ijms23105434>.
 109. Sobczyk-Guzenda A., Boniecka P., Laska-Lesniewicz A., Makowka M., Szymanowski H. Micro- and Nanoparticulate Hydroxyapatite Powders as Fillers in Polyacrylate Bone Cement-A Comparative Study. *Materials (Basel)* 2020; 13(12):2736. <https://doi.org/10.3390/ma13122736>.
 110. Gao C., Peng S., Feng P. et al. Bone biomaterials and interactions with stem cells. *Bone Res* 2017; 5, 17059. <https://doi.org/10.1038/boneres.2017.59>
 111. Zimmermann E.A., Ritchie R.O. Bone as a Structural Material. *Adv Healthc Mater* 2015; 4(9):1287-304. <https://doi.org/10.1002/adhm.201500070>.
 112. Kien P.T., Phu H.D., Linh N.V.V., Quyen T.N., Hoa N.T. Recent Trends in Hydroxyapatite (HA) Synthesis and the Synthesis Report of Nanostructure HA by Hydrothermal Reaction. *Adv Exp Med Biol* 2018; 1077:343-354. https://doi.org/10.1007/978-981-13-0947-2_18.
 113. Fadil N.A. Synthesis Techniques of Bioceramic Hydroxyapatite for Biomedical Applications. *Journal of Biomimetics, Biomaterials and Biomedical Engineering* 2023; 59:59-80. <https://doi.org/10.4028/p-yqw75e>.
 114. Clabel H., J. L., Awan I., Pinto A., Nogueira I., Bezzon V., Leite E. & Balogh D., Mastelaro V., Ferreira S., Marega E. Insights on the mechanism of solid state reaction between TiO₂ and BaCO₃ to produce BaTiO₃ powders: The role of calcination, milling, and mixing solvent. *Ceramics International* 2019; 46(3):2987-3001. <https://doi.org/10.1016/j.ceramint.2019.09.296>

115. Sathiyavimal S., Vasantharaj S., LewisOscar F., Selvaraj R., Brindhadevi K., Pugazhendhi A. Natural organic and inorganic hydroxyapatite biopolymer composite for biomedical applications. *Progress in Organic Coatings* 2020; 147, 105858. <https://doi.org/10.1016/j.porgcoat.2020.105858>
116. Szczes A., Hołysz L., Chibowski E. Synthesis of hydroxyapatite for biomedical applications. *Adv Colloid Interface Sci* 2017; 249:321-330. <https://doi.org/10.1016/j.cis.2017.04.007>.
117. Chesley M., Kennard R., Roozbahani S., Kim S.M., Kuk K., Mason M. One-step hydrothermal synthesis with in situ milling of biologically relevant hydroxyapatite. *Mater Sci Eng C Mater Biol Appl* 2020; 113:110962. <https://doi.org/10.1016/j.msec.2020.110962>.
118. Fihri A., Len C., Varma R., Solhy A. Hydroxyapatite: A review of syntheses, structure and applications in heterogeneous catalysis. *Coordination Chemistry Reviews* 2017; 347:48-76. <https://dx.doi.org/10.1016/j.ccr.2017.06.009>
119. Qi M.L., He K., Huang Z.N. et al. Hydroxyapatite Fibers: A Review of Synthesis Methods 2017; *JOM* 69, 1354-1360. <https://doi.org/10.1007/s11837-017-2427-2>
120. Andrés N.C., D'Elia N.L., Ruso J.M., Campelo A.E., Massheimer V.L., Messina P.V. Manipulation of Mg²⁺-Ca²⁺ Switch on the Development of Bone Mimetic Hydroxyapatite. *ACS Appl Mater Interfaces* 2017; 9(18):15698-15710. <https://doi.org/10.1021/acsami.7b02241>.
121. Lala S., Ghosh M., Das P.K., Kar T., Pradhan S.K. Mechanical preparation of nanocrystalline biocompatible single-phase Mn-doped A-type carbonated hydroxyapatite (A-cHAp): effect of Mn doping on microstructure. *Dalton Trans* 2015; 44(46):20087-97. <https://doi.org/10.1039/c5dt03398e>.
122. Wang M., Wang L., Shi C., Sun T., Zeng Y., Zhu Y. The crystal structure and chemical state of aluminum-doped hydroxyapatite by experimental and first principles calculation studies. *Phys Chem Chem Phys* 2016; 18(31):21789-96. <https://doi.org/10.1039/c6cp03230c>.
123. Kolmas J., Kuras M., Oledzka E., Sobczak M. A solid-state NMR study of selenium substitution into nanocrystalline hydroxyapatite. *Int J Mol Sci* 2015; 16(5):11452-64. <https://doi.org/10.3390/ijms160511452>.
124. Lin D.J., Lin H.L., Haung S.M., Liu S.M., Chen W.C. Effect of pH on the In Vitro Biocompatibility of Surfactant-Assisted Synthesis and Hydrothermal Precipitation of Rod-Shaped Nano-Hydroxyapatite. *Polymers (Basel)* 2021; 13(17):2994. <https://doi.org/10.3390/polym13172994>.
125. Lee I.-H., Lee J.-A., Lee J.-H., Heo Y.-W., Kim J.-J. Effects of pH and reaction temperature on hydroxyapatite powders synthesized by precipitation. *Journal of the Korean Ceramic Society* 2019; 57:56-64. <https://doi.org/10.1007/s43207-019-00004-0>
126. Wijesinghe W.P., Mantilaka M.M., Premalal E.V., Herath H.M., Mahalingam S., Edirisinghe M., Rajapakse R.P., Rajapakse R.M. Facile synthesis of both needle-like and spherical hydroxyapatite nanoparticles: effect of synthetic temperature and calcination on morphology, crystallite size and crystallinity. *Mater Sci Eng C Mater Biol Appl* 2014; 42:83-90. <https://doi.org/10.1016/j.msec.2014.05.032>.
127. Boyd A.R., Rutledge L., Randolph L.D., Meenan B.J. Strontium-substituted hydroxyapatite coatings deposited via a co-deposition sputter technique. *Mater Sci Eng C Mater Biol Appl* 2015; 46:290-300. <https://doi.org/10.1016/j.msec.2014.10.046>.
128. Robinson L., Salma-Ancane K., Stipniece L., Meenan B.J., Boyd A.R. The deposition of strontium and zinc Co-substituted hydroxyapatite coatings. *J Mater Sci Mater Med* 2017; 28:51. <https://doi.org/10.1007/s10856-017-5846-2>.
129. Gu M., Li W., Jiang L., Li X. Recent progress of rare earth doped hydroxyapatite nanoparticles: Luminescence properties, synthesis and biomedical applications. *Acta Biomater* 2022; 148:22-43. <https://doi.org/10.1016/j.actbio.2022.06.006>.
130. LaKrat M., Jodati H., Mejdoubi E., Evis Z. Synthesis and characterization of pure and Mg, Cu, Ag, and Sr doped calcium-deficient hydroxyapatite from brushite as precursor using the dissolution-precipitation method. *Powder Technology* 2022; 413, 118026. <https://doi.org/10.1016/j.powtec.2022.118026>
131. Shah R.K., Fahmi M.N., Mat A.H., Zainal A.A. The synthesis of hydroxyapatite through the precipitation method. *Med J Malaysia* 2004; 59 Suppl B:75-6.
132. Chen W., Nichols L., Brinkley F., Bohna K., Tian W., Priddy M.W., Priddy L.B. Alkali treatment facilitates functional nano-hydroxyapatite coating of 3D printed polylactic acid scaffolds. *Mater Sci Eng C Mater Biol Appl* 2021; 120:111686. <https://doi.org/10.1016/j.msec.2020.111686>.
133. Enami H., Nakahara I., Ando W., Uemura K., Hamada H., Takao M., Sugano N. Osteocompatibility of Si₃N₄-coated carbon fiber-reinforced polyetheretherketone (CFRP) and hydroxyapatite-coated CFRP with antibiotics and antithrombotic drugs. *J Artif Organs* 2023; 26(2):144-150. <https://doi.org/10.1007/s10047-022-01340-5>.
134. Yudyanto Y., Utomo J., Rosita R. R., Ariyanto L. P., Fathurochman F., Nasikhudin N., Hartatiek H. Porosity, hardness and microstructure of nano-hydroxyapatite/PEG composite synthesized by co-precipitation temperature variations. *AIP Conference Proceedings* 2023; 2748 (1): 020002. <https://doi.org/10.1063/5.0138576>

135. Chen J., Yang Y., Etim I.P., Tan L., Yang K., Misra R.D.K., Wang J., Su X. Recent Advances on Development of Hydroxyapatite Coating on Biodegradable Magnesium Alloys: A Review. *Materials* (Basel) 2021; 14(19):5550. <https://doi.org/10.3390/ma14195550>.
136. Kalpana M., Nagalakshmi R. Nano Hydroxyapatite for Biomedical Applications Derived from Chemical and Natural Sources by Simple Precipitation Method. *Appl Biochem Biotechnol* 2023; 195(6):3994-4010. <https://doi.org/10.1007/s12010-022-03968-8>.
137. Kuśmierczyk F., Fiołek A., Łukaszczuk A., Kopia A., Sitarz M., Zimowski S., Cieniek Ł., Moskalewicz T. Microstructure and Selected Properties of Advanced Biomedical n-HA/ZnS/Sulfonated PEEK Coatings Fabricated on Zirconium Alloy by Duplex Treatment. *Int J Mol Sci* 2022; 23(6):3244. <https://doi.org/10.3390/ijms23063244>.
138. Hu H., Lin C., Leng Y. [An investigation of HAP/organic polymer composite coating prepared by electrochemical co-deposition technique (II) characterization of XRD, SEM and mechanic properties]. *Sheng Wu Yi Xue Gong Cheng Xue Za Zhi* 2003; 20(2):202-4, 236. Chinese.
139. Zhang Y., Dong K., Wang F., Wang H., Wang J., Jiang Z., Diao S. Three dimensional macroporous hydroxyapatite/chitosan foam-supported polymer micelles for enhanced oral delivery of poorly soluble drugs. *Colloids Surf B Biointerfaces* 2018; 170:497-504. <https://doi.org/10.1016/j.colsurfb.2018.06.053>.
140. Sivasankari S., Kalaivizhi R., Gowriboy N., Ganesh M.R., Shazia Anjum M. Hydroxyapatite integrated with cellulose acetate/polyetherimide composite membrane for biomedical applications. *Polymer Composites* 2021; 42(10):5512-5526. <https://doi.org/10.1002/pc.26242>
141. Akiyama N., Patel K.D., Jang E.J., Shannon M.R., Patel R., Patel M., Perriman A.W. Tubular nanomaterials for bone tissue engineering. *J Mater Chem B* 2023; 11(27):6225-6248. <https://doi.org/10.1039/d3tb00905j>.
142. Adamu D. B. et al. Synthesis and characterization of bismuth-doped hydroxyapatite nanorods for fluoride removal. *Environmental Advances* 2023; 12:100360. <https://doi.org/10.1016/j.envadv.2023.100360>
143. Asri R.I., Harun W.S., Hassan M.A., Ghani S.A., Buyong Z. A review of hydroxyapatite-based coating techniques: Sol-gel and electrochemical depositions on biocompatible metals. *J Mech Behav Biomed Mater* 2016; 57:95-108. <https://doi.org/10.1016/j.jmbbm.2015.11.031>.
144. Kuo M. C., Yen S. K. The process of electrochemical deposited hydroxyapatite coatings on biomedical titanium at room temperature," *Materials Science and Engineering C* 2002; 20(1-2):153-160. [https://doi.org/10.1016/S0928-4931\(02\)00026-7](https://doi.org/10.1016/S0928-4931(02)00026-7)
145. Kumar S., Gupta R.K., Archana K. et al. Development of Ternary Hydroxyapatite-Al₂O₃-TiO₂ Nanocomposite Coating on Mg Alloy by Electrophoretic Deposition Method. *J. of Mater Eng and Perform* 2023. <https://doi.org/10.1007/s11665-023-08290-w>
146. Baheti W., Lv S., Mila, Ma L., Amantai D., Sun H., He H. Graphene/hydroxyapatite coating deposit on titanium alloys for implant application. *J Appl Biomater Funct Mater* 2023; 21:22808000221148104. <https://doi.org/10.1177/22808000221148104>.
147. Elias L., Hegde A.C. Electrodeposited Metallic/Nanocomposite Coatings. *Advances in Corrosion Control of Magnesium and its Alloys*. CRC Press. C. 243-261. <https://doi.org/10.1201/9781003319856>
148. Li G., Song Y., Chen X., Xu W., Tong G., Zhang L., Li J., Zhu X. Preparation, Corrosion Behavior and Biocompatibility of MgFe-Layered Double Hydroxides and Calcium Hydroxyapatite Composite Films on 316 L Stainless Steel. *Materials Today Communications* 2022; 34:105195. <https://doi.org/10.1016/j.mtcomm.2022.105195>
149. Sundaramali G., Aiyasamy J., Karthikeyan S., Kandavel T., Arulmurugan B., Rajkumar S., Sharma S., Li C., Dwivedi S., Kumar A., Singh R., Eldin S. Experimental investigations of electrodeposited Zn-Ni, Zn-Co, and Ni-Cr-Co-based novel coatings on AA7075 substrate to ameliorate the mechanical, abrasion, morphological, and corrosion properties for automotive applications. *Reviews on advanced materials science* 2023; 62(1):20220324. <https://doi.org/10.1515/rams-2022-0324>
150. Al-Noaman A., Rawlinson S. C. F. Polyether ether ketone coated with nanohydroxyapatite/graphene oxide composite promotes bioactivity and antibacterial activity at the surface of the material. *European Journal of Oral Sciences* 2023; e12946. <https://doi.org/10.1111/eos.12946>
151. Gao Q., Zhang L., Chen Y., Nie H., Zhang B., Li H. Interfacial Design and Construction of Carbon Fiber Composites by Strongly Bound Hydroxyapatite Nanobelt-Carbon Nanotubes for Biological Applications. *ACS Appl Bio Mater* 2023; 6(2):874-882. <https://doi.org/10.1021/acsabm.2c01028>.
152. Park S.J., Jang J.M. Electrodeposition of hydroxyapatite nanoparticles onto ultra-fine TiO₂ nanotube layer by electrochemical reaction in mixed electrolyte. *J Nanosci Nanotechnol* 2011; 11(8):7167-71. <https://doi.org/10.1166/jnn.2011.4865>.
153. Zhang Q., Qiang L., Liu Y., Fan M., Si X., Zheng P. Biomaterial-assisted tumor therapy: A brief review of hydroxyapatite nanoparticles and its composites used in bone tumors therapy. *Front Bioeng Biotechnol* 2023; 11:1167474. <https://doi.org/10.3389/fbioe.2023.1167474>.
154. Kargozar S., Mollazadeh S., Kermani F., Webster T.J., Nazarnezhad S., Hamzehlou S., Baino F. Hydroxyapatite Nanoparticles for Improved Cancer Theranostics. *J Funct Biomater* 2022; 13(3):100. <https://doi.org/10.3390/jfb13030100>.

155. Gómora-Figueroa A. P. et al. Oil emulsions in naturally fractured Porous Media .Petroleum 2019; 5(3):215-226. <https://doi.org/10.1016/j.petlm.2018.12.004>
156. Liang Q. et al. Surfactant-assisted synthesis of photocatalysts: Mechanism, synthesis, recent advances and environmental application. Chemical engineering journal 2019; 372:429-451. <https://doi.org/10.1016/j.cej.2019.04.168>
157. Sadat-Shojai M., Khorasani M.T., Dinpanah-Khoshdargi E., Jamshidi A. Synthesis methods for nanosized hydroxyapatite with diverse structures. Acta Biomater 2013; 9(8):7591-621. <https://doi.org/10.1016/j.actbio.2013.04.012>.
158. Ioişescu A. et al. Synthesis and characterization of hydroxyapatite obtained from different organic precursors by sol-gel method. Journal of thermal analysis and calorimetry 2009; 96(3):937-942. <https://doi.org/10.1007/s10973-009-0044-1>
159. Yun Y.H., Lee J.K. Sol-Gel Coating of Hydroxyapatite on Zirconia Substrate. J Nanosci Nanotechnol 2021; 21(8):4169-4173. <https://doi.org/10.1166/jnn.2021.19375>.
160. Jaafar A., Hecker C., Árki P., Joseph Y. Sol-Gel Derived Hydroxyapatite Coatings for Titanium Implants: A Review. Bioengineering (Basel) 2020; 7(4):127. <https://doi.org/10.3390/bioengineering7040127>.
161. Ishikawa K., Garskaite E., Kareiva A. Sol-gel synthesis of calcium phosphate-based biomaterials—A review of environmentally benign, simple, and effective synthesis routes. Journal of Sol-Gel Science and Technology 2020; 94:551-572. <https://doi.org/10.1007/s10971-020-05245-8>
162. Molino G. et al. Biomimetic and mesoporous nano-hydroxyapatite for bone tissue application: A short review. Biomedical Materials 2020; 15(2):022001. <https://doi.org/10.1088/1748-605X/ab5f1a>
163. Hernández-Barreto D.F., Hernández-Cocoletzi H., Moreno-Piraján J.C. Biogenic Hydroxyapatite Obtained from Bone Wastes Using CO₂-Assisted Pyrolysis and Its Interaction with Glyphosate: A Computational and Experimental Study. ACS Omega 2022; 7(27):23265-23275. <https://doi.org/10.1021/acsomega.2c01379>.
164. Amna T. Valorization of Bone Waste of Saudi Arabia by Synthesizing Hydroxyapatite. Appl Biochem Biotechnol 2018; 186(3):779-788. <https://doi.org/10.1007/s12010-018-2768-5>.
165. Wu S.C., Hsu H.C., Wang H.F., Liou S.P., Ho W.F. Synthesis and Characterization of Nano-Hydroxyapatite Obtained from Eggshell via the Hydrothermal Process and the Precipitation Method. Molecules 2023; 28(13):4926. <https://doi.org/10.3390/molecules28134926>.
166. Patel D.K., Jin B., Dutta S.D., Lim K.T. Osteogenic potential of human mesenchymal stem cells on eggshells-derived hydroxyapatite nanoparticles for tissue engineering. J Biomed Mater Res B Appl Biomater 2020; 108(5):1953-1960. <https://doi.org/10.1002/jbm.b.34536>.
167. Prado J.P.D.S., Yamamura H., Magri A.M.P., Ruiz P.L.M., Prado J.L.D.S., Rennó A.C.M., Ribeiro D.A., Granito R.N. In vitro and in vivo biological performance of hydroxyapatite from fish waste. J Mater Sci Mater Med 2021; 32(9):109. <https://doi.org/10.1007/s10856-021-06591-x>.
168. Ahmed H.Y., Safwat N., Shehata R., Althubaiti E.H., Kareem S., Atef A., Qari S.H., Aljahani A.H., Al-Meshal A.S., Youssef M., Sami R. Synthesis of Natural Nano-Hydroxyapatite from Snail Shells and Its Biological Activity: Antimicrobial, Antibiofilm, and Biocompatibility. Membranes (Basel) 2022; 12(4):408. <https://doi.org/10.3390/membranes12040408>.
169. Granito R.N., Muniz Renno A.C., Yamamura H., de Almeida M.C., Menin Ruiz P.L., Ribeiro D.A. Hydroxyapatite from Fish for Bone Tissue Engineering: A Promising Approach. Int J Mol Cell Med 2018; 7(2):80-90. <https://doi.org/10.22088/IJMCM.BUMS.7.2.80>.
170. Kodali D., Hembrick-Holloman V., Gunturu D.R., Samuel T., Jeelani S., Rangari V.K. Influence of Fish Scale-Based Hydroxyapatite on Forcespun Polycaprolactone Fiber Scaffolds. ACS Omega 2022; 7(10):8323-8335. <https://doi.org/10.1021/acsomega.1c05593>.
171. Shaltout A.A., Allam M.A., Moharram M.A. FTIR spectroscopic, thermal and XRD characterization of hydroxyapatite from new natural sources. Spectrochim Acta A Mol Biomol Spectrosc 2011; 83(1):56-60. <https://doi.org/10.1016/j.saa.2011.07.036>.
172. Pradeep S., Jain A.S., Dharmashekara C., Prasad S.K., Akshatha N., Pruthvish R., Amachawadi R.G., Srinivasa C., Syed A., Elgorban A.M., Al Kheraif A.A., Ortega-Castro J., Frau J., Flores-Holguín N., Shivamallu C., Kollur S.P., Glossman-Mitnik D. Synthesis, Computational Pharmacokinetics Report, Conceptual DFT-Based Calculations and Anti-Acetylcholinesterase Activity of Hydroxyapatite Nanoparticles Derived From *Acorus Calamus* Plant Extract. Front Chem. 2021; 9:741037. <https://doi.org/10.3389/fchem.2021.741037>.
173. Ghate P., Prabhu S.D., Murugesan G., Goveas L.C., Varadavenkatesan T., Vinayagam R., Lan Chi N.T., Pugazhendhi A., Selvaraj R. Synthesis of hydroxyapatite nanoparticles using *Acacia falcata* leaf extract and study of their anti-cancerous activity against cancerous mammalian cell lines. Environ Res 2022; 214(Pt 2):113917. <https://doi.org/10.1016/j.envres.2022.113917>.
174. Susanto H. et al. The Characterization of Green Materials of Moringa oleifera Leaf Powder (MOLP) from Madura Island with Different Preparation Methods. IOP Conference Series: Earth and Environmental Science. IOP Publishing 2019; 276(1):012005. <https://doi.org/10.1088/1755-1315/276/1/012005>

175. Domene-López D., Delgado-Marín J.J., Martín-Gullón I., García-Quesada J.C., Montalbán M.G. Comparative study on properties of starch films obtained from potato, corn and wheat using 1-ethyl-3-methylimidazolium acetate as plasticizer. *Int J Biol Macromol* 2019; 135:845-854. <https://doi.org/10.1016/j.ijbiomac.2019.06.004>.
176. Khlestkin V.K., Rozanova I.V., Efimov V.M., Khlestkina E.K. Starch phosphorylation associated SNPs found by genome-wide association studies in the potato (*Solanum tuberosum* L.). *BMC Genet.* 2019; 20(Suppl 1):29. <https://doi.org/10.1186/s12863-019-0729-9>.
177. Manoj M. et al. A plant-mediated synthesis of nanostructured hydroxyapatite for biomedical applications: a review. *RSC advances* 2020; 10(67):40923-40939. <https://doi.org/10.1039/D0RA08529D>
178. Luo M., Li Z., Su M., Gadd G.M., Yin Z., Benton M.J., Pan Y., Zheng D., Zhao T., Li Z., Chen Y. Fungal-induced fossil biomineralization. *Curr Biol* 2023; 33(12):2417-2424.e2. <https://doi.org/10.1016/j.cub.2023.04.067>.
179. Shi D., Tong H., Lv M., Luo D., Wang P., Xu X., Han Z. Optimization of hydrothermal synthesis of hydroxyapatite from chicken eggshell waste for effective adsorption of aqueous Pb(II). *Environ Sci Pollut Res Int* 2021; 28(41):58189-58205. <https://doi.org/10.1007/s11356-021-14772-y>.
180. Barakat N. A. M. et al. Physicochemical characterizations of hydroxyapatite extracted from bovine bones by three different methods: extraction of biologically desirable HAp //Materials Science and Engineering: C 2008; 28(8):1381-1387. <https://doi.org/10.1016/j.msec.2008.03.003>
181. Boudreau S. et al. Isolation of hydroxyapatite from Atlantic salmon processing waste using a protease and lipase mixture. *RSC Sustainability* 2023. <https://doi.org/10.1039/D3SU00102D>
182. Mohd Pu'ad N.A.S., Koshy P., Abdullah H.Z., Idris M.I., Lee T.C. Syntheses of hydroxyapatite from natural sources. *Heliyon* 2019; 5(5):e01588. <https://doi.org/10.1016/j.heliyon.2019.e01588>.
183. Forero-Sossa P.A., Salazar-Martínez J.D., Giraldo-Betancur A.L., Segura-Giraldo B., Restrepo-Parra E. Temperature effect in physicochemical and bioactive behavior of biogenic hydroxyapatite obtained from porcine bones. *Sci Rep* 2021; 11(1):11069. <https://doi.org/10.1038/s41598-021-89776-2>.
184. Horta M. K. S. et al. Hydroxyapatite from biowaste for biomedical applications: obtainment, characterization and in vitro assays. *Materials Research* 2023; 26:e20220466. <https://doi.org/10.1590/1980-5373-MR-2022-0466>
185. Joschek S., Nies B., Krotz R., Göferich A. Chemical and physicochemical characterization of porous hydroxyapatite ceramics made of natural bone. *Biomaterials* 2000; 21(16):1645-58. [https://doi.org/10.1016/S0142-9612\(00\)00036-3](https://doi.org/10.1016/S0142-9612(00)00036-3).
186. Cao X., Zhu J., Zhang C., Xian J., Li M., Nath Varma S., Qin Z., Deng Q., Zhang X., Yang W., Liu C. Magnesium-Rich Calcium Phosphate Derived from Tilapia Bone Has Superior Osteogenic Potential. *J Funct Biomater* 2023; 14(7):390. <https://doi.org/10.3390/jfb14070390>.
187. Gani M.A., Budiatin A.S., Lestari M.L.A.D., Rantam F.A., Ardianto C., Khotib J. Fabrication and Characterization of Submicron-Scale Bovine Hydroxyapatite: A Top-Down Approach for a Natural Biomaterial. *Materials (Basel)* 2022; 15(6):2324. <https://doi.org/10.3390/ma15062324>.
188. Lee M.C., Seonwoo H., Jang K.J., Pandey S., Lim J., Park S., Kim J.E., Choung Y.H., Garg P., Chung J.H. Development of novel gene carrier using modified nano hydroxyapatite derived from equine bone for osteogenic differentiation of dental pulp stem cells. *Bioact Mater* 2021; 6(9):2742-2751. <https://doi.org/10.1016/j.bioactmat.2021.01.020>.
189. Yamamura H., da Silva V.H.P., Ruiz P.L.M., Ussui V., Lazar D.R.R., Renno A.C.M., Ribeiro D.A. Physicochemical characterization and biocompatibility of hydroxyapatite derived from fish waste. *J Mech Behav Biomed Mater* 2018; 80:137-142. <https://doi.org/10.1016/j.jmbbm.2018.01.035>.
190. Acharya P., Kupendra M., Fasim A., Anantharaju K.S., Kottam N., Murthy V.K., More S.S. Synthesis of nano hydroxyapatite from Hypophthalmichthys molitrix (silver carp) bone waste by two different methods: a comparative biophysical and in vitro evaluation on osteoblast MG63 cell lines. *Biotechnol Lett* 2022; 44(10):1175-1188. <https://doi.org/10.1007/s10529-022-03292-5>.
191. Mathirat A., Dalavi P.A., Prabhu A., Yashaswini Devi G.V., Anil S., Senthilkumar K., Seong G.H., Sargod S.S., Bhat S.S., Venkatesan J. Remineralizing Potential of Natural Nano-Hydroxyapatite Obtained from *Epinephelus chlorostigma* in Artificially Induced Early Enamel Lesion: An In Vitro Study. *Nanomaterials (Basel)* 2022; 12(22):3993. <https://doi.org/10.3390/nano12223993>.
192. Athinarayanan J., Periasamy V.S., Alshatwi A.A. Simultaneous fabrication of carbon nanodots and hydroxyapatite nanoparticles from fish scale for biomedical applications. *Mater Sci Eng C Mater Biol Appl* 2020; 117:111313. <https://doi.org/10.1016/j.msec.2020.111313>.
193. Baek J.W., Kim K.S., Park H., Kim B.S. Marine plankton exoskeleton-derived hydroxyapatite/polycaprolactone composite 3D scaffold for bone tissue engineering. *Biomater Sci* 2022; 10(24):7055-7066. <https://doi.org/10.1039/d2bm00875k>.
194. Palaveniene A., Tamburaci S., Kimna C., Glambaite K., Baniukaitiene O., Tihminlioglu F., Liesiene J. Osteoconductive 3D porous composite scaffold from regenerated cellulose and cuttlebone-derived hydroxyapatite. *J Biomater Appl* 2019; 33(6):876-890. <https://doi.org/10.1177/0885328218811040>.

195. Fatimah I., Hidayat H., Purwiandono G., Khoirunisa K., Zahra H.A., Audita R., Sagadevan S. Green Synthesis of Antibacterial Nanocomposite of Silver Nanoparticle-Doped Hydroxyapatite Utilizing *Curcuma longa* Leaf Extract and Land Snail (*Achatina fulica*) Shell Waste. J Funct Biomater 2022; 13(2):84. <https://doi.org/10.3390/jfb13020084>.
196. Mebarki M., Coquelin L., Layrolle P., Battaglia S., Tossou M., Hernigou P., Rouard H., Chevallier N. Enhanced human bone marrow mesenchymal stromal cell adhesion on scaffolds promotes cell survival and bone formation. Acta Biomater 2017; 59:94-107. <https://doi.org/10.1016/j.actbio.2017.06.018>.
197. Ferraz M.P. Bone Grafts in Dental Medicine: An Overview of Autografts, Allografts and Synthetic Materials. Materials (Basel) 2023; 16(11):4117. <https://doi.org/10.3390/ma16114117>.
198. Gibson I.R., Bonfield W. Novel synthesis and characterization of an AB-type carbonate-substituted hydroxyapatite. J Biomed Mater Res 2002; 59(4):697-708. <https://doi.org/10.1002/jbm.10044>.
199. Siddiqi S.A., Azhar U. 6 - Carbonate Substituted Hydroxyapatite. Elsevier Ltd 2020; 149-173. <https://doi.org/10.1016/B978-0-08-102834-6.00006-9>
200. Ishikawa K., Miyamoto Y., Tsuchiya A., Hayashi K., Tsuru K., Ohe G. Physical and Histological Comparison of Hydroxyapatite, Carbonate Apatite, and β -Tricalcium Phosphate Bone Substitutes. Materials (Basel) 2018; 11(10):1993. <https://doi.org/10.3390/ma11101993>.
201. Everts V., Delaissé J.M., Korper W., Jansen D.C., Tigchelaar-Gutter W., Saftig P., Beertsen W. The bone lining cell: its role in cleaning Howship's lacunae and initiating bone formation. J Bone Miner Res 2002; 17(1):77-90. <https://doi.org/10.1359/jbmr.2002.17.1.77>.
202. Carrodeguas R.G., De Aza S. α -Tricalcium phosphate: synthesis, properties and biomedical applications. Acta Biomater 2011; 7(10):3536-46. <https://doi.org/10.1016/j.actbio.2011.06.019>.
203. Crespi R., Cappare P., Gherlone E. Magnesium-enriched hydroxyapatite compared to calcium sulfate in the healing of human extraction sockets: radiographic and histomorphometric evaluation at 3 months. J Periodontol 2009; 80(2):210-8. <https://doi.org/10.1902/jop.2009.080400>.
204. Atilgan S. et al. An experimental comparison of the effects of calcium sulfate particles and β -tricalcium phosphate/hydroxyapatite granules on osteogenesis in internal bone cavities. Biotechnology & Biotechnological Equipment 2007; 21(2):205-210. <https://doi.org/10.1080/13102818.2007.10817446>
205. Chen F., Wang M., Wang J., Chen X., Li X., Xiao Y., Zhang X. Effects of hydroxyapatite surface nano/micro-structure on osteoclast formation and activity. J Mater Chem B 2019; 7(47):7574-7587. <https://doi.org/10.1039/c9tb01204d>.
206. Matsumoto M.A., Caviquioli G., Bigueti C.C., Holgado Lde A., Saraiva P.P., Rennó A.C., Kawakami R.Y. A novel bioactive vitroceramic presents similar biological responses as autogenous bone grafts. J Mater Sci Mater Med 2012; 23(6):1447-56. <https://doi.org/10.1007/s10856-012-4612-8>.
207. Bellucci D., Anesi A., Salvatori R., Chiarini L., Cannillo V. A comparative in vivo evaluation of bioactive glasses and bioactive glass-based composites for bone tissue repair. Mater Sci Eng C Mater Biol Appl 2017; 79:286-295. <https://doi.org/10.1016/j.msec.2017.05.062>.
208. Bellucci D., Braccini S., Chiellini F., Balasubramanian P., Boccaccini A.R., Cannillo V. Bioactive glasses and glass-ceramics versus hydroxyapatite: Comparison of angiogenic potential and biological responsiveness. J Biomed Mater Res A 2019; 107(12):2601-2609. <https://doi.org/10.1002/jbm.a.36766>.
209. Souza E.Q.M., Costa Klaus A.E., Espósito Santos B.F., Carvalho da Costa M., Ervolino E., Coelho de Lima D., Fernandes L.A. Evaluations of hydroxyapatite and bioactive glass in the repair of critical size bone defects in rat calvaria. J Oral Biol Craniofac Res 2020; 10(4):422-429. <https://doi.org/10.1016/j.jobcr.2020.07.014>.
210. Hayman A.R. Tartrate-resistant acid phosphatase (TRAP) and the osteoclast/immune cell dichotomy. Autoimmunity 2008; 41(3):218-23. <https://doi.org/10.1080/08916930701694667>.
211. de Melo Pereira D., Davison N., Habibović P. Human osteoclast formation and resorptive function on biomaterialized collagen. Bioact Mater 2021; 8:241-252. <https://doi.org/10.1016/j.bioactmat.2021.06.036>.
212. Tayton E., Purcell M., Aarvold A., Smith J.O., Briscoe A., Kanczler J.M., Shakesheff K.M., Howdle S.M., Dunlop D.G., Oreffo R.O. A comparison of polymer and polymer-hydroxyapatite composite tissue engineered scaffolds for use in bone regeneration. An in vitro and in vivo study. J Biomed Mater Res A 2014; 102(8):2613-24. <https://doi.org/10.1002/jbm.a.34926>.
213. Yang W., Both S.K., Zuo Y., Birgani Z.T., Habibovic P., Li Y., Jansen J.A., Yang F. Biological evaluation of porous aliphatic polyurethane/hydroxyapatite composite scaffolds for bone tissue engineering. J Biomed Mater Res A 2015; 103(7):2251-9. <https://doi.org/10.1002/jbm.a.35365>.
214. Deng X., Huang B., Hu R., Chen L., Tang Y., Lu C., Chen Z., Zhang W., Zhang X. 3D printing of robust and biocompatible poly(ethylene glycol)diacrylate/nano-hydroxyapatite composites via continuous liquid interface production. J Mater Chem B 2021; 9(5):1315-1324. <https://doi.org/10.1039/d0tb02182b>.
215. Ielo I., Calabrese G., De Luca G., Conoci S. Recent Advances in Hydroxyapatite-Based Biocomposites for Bone Tissue Regeneration in Orthopedics. Int J Mol Sci 2022; 23(17):9721. <https://doi.org/10.3390/ijms23179721>.

216. Sun J.S., Lin F.H., Hung T.Y., Tsuang Y.H., Chang W.H., Liu H.C. The influence of hydroxyapatite particles on osteoclast cell activities. *J Biomed Mater Res* 1999; 45(4):311-21. [https://doi.org/10.1002/\(sici\)1097-4636\(19990615\)45:4<311::aid-jbm5>3.0.co;2-9](https://doi.org/10.1002/(sici)1097-4636(19990615)45:4<311::aid-jbm5>3.0.co;2-9).
217. Han Y., Li S., Cao X., Yuan L., Wang Y., Yin Y., Qiu T., Dai H., Wang X. Different inhibitory effect and mechanism of hydroxyapatite nanoparticles on normal cells and cancer cells in vitro and in vivo. *Sci Rep* 2014; 4:7134. <https://doi.org/10.1038/srep07134>.
218. Narducci P., Nicolin V. Differentiation of activated monocytes into osteoclast-like cells on a hydroxyapatite substrate: an in vitro study. *Ann Anat* 2009; 191(4):349-55. <https://doi.org/10.1016/j.aanat.2009.02.009>.
219. Veillat V., Spuul P., Daubon T., Egaña I., Kramer I., Génot E. Podosomes: Multipurpose organelles? *Int J Biochem Cell Biol* 2015; 65:52-60. <https://doi.org/10.1016/j.biocel.2015.05.020>.
220. Zhang K., Zhou Y., Xiao C., Zhao W., Wu H., Tang J., Li Z., Yu S., Li X., Min L., Yu Z., Wang G., Wang L., Zhang K., Yang X., Zhu X., Tu C., Zhang X. Application of hydroxyapatite nanoparticles in tumor-associated bone segmental defect. *Sci Adv*. 2019; 5(8):eaax6946. <https://doi.org/10.1126/sciadv.aax6946>.
221. Chen Z., Deng J., Cao J., Wu H., Feng G., Zhang R., Ran B., Hu K., Cao H., Zhu X., Zhang X. Nano-hydroxyapatite-evoked immune response synchronized with controllable immune adjuvant release for strengthening melanoma-specific growth inhibition. *Acta Biomater* 2022; 145:159-171. <https://doi.org/10.1016/j.actbio.2022.04.002>.
222. Ding X., Takahata M., Akazawa T., Iwasaki N., Abe Y., Komatsu M., Murata M., Ito M., Abumi K., Minami A. Improved bioabsorbability of synthetic hydroxyapatite through partial dissolution-precipitation of its surface. *J Mater Sci Mater Med* 2011; 22(5):1247-55. <https://doi.org/10.1007/s10856-011-4291-x>.
223. Mestres G., Espanol M., Xia W., Persson C., Ginebra M.P., Ott M.K. Inflammatory response to nano- and microstructured hydroxyapatite. *PLoS One* 2015; 10(3):e0120381. <https://doi.org/10.1371/journal.pone.0120381>.
224. Lebre F., Sridharan R., Sawkins M.J., Kelly D.J., O'Brien F.J., Lavelle E.C. The shape and size of hydroxyapatite particles dictate inflammatory responses following implantation. *Sci Rep* 2017; 7(1):2922. <https://doi.org/10.1038/s41598-017-03086-0>.
225. Ghanaati S., Udeabor S.E., Barbeck M., Willershausen I., Kuenzel O., Sader R.A., Kirkpatrick C.J. Implantation of silicon dioxide-based nanocrystalline hydroxyapatite and pure phase beta-tricalciumphosphate bone substitute granules in caprine muscle tissue does not induce new bone formation. *Head Face Med* 2013; 9:1. <https://doi.org/10.1186/1746-160X-9-1>.
226. Li C., Yang L., Ren X., Lin M., Jiang X., Shen D., Xu T., Ren J., Huang L., Qing W., Zheng J., Mu Y. Groove structure of porous hydroxyapatite scaffolds (HAS) modulates immune environment via regulating macrophages and subsequently enhances osteogenesis. *J Biol Inorg Chem* 2019; 24(5):733-745. <https://doi.org/10.1007/s00775-019-01687-w>.
227. Zeng Q., Wang R., Hua Y., Wu H., Chen X., Xiao Y.C., Ao Q., Zhu X., Zhang X. Hydroxyapatite nanoparticles drive the potency of Toll-like receptor 9 agonist for amplified innate and adaptive immune response. *Nano Res* 2022; 15(10):9286-9297. <https://doi.org/10.1007/s12274-022-4683-x>.
228. Zhang L., Liang Z., Chen C., Yang X., Fu D., Bao H., Li M., Shi S., Yu G., Zhang Y., Zhang C., Zhang W., Xue C., Sun B. Engineered Hydroxyapatite Nanoadjuvants with Controlled Shape and Aspect Ratios Reveal Their Immunomodulatory Potentials. *ACS Appl Mater Interfaces* 2021; 13(50):59662-59672. <https://doi.org/10.1021/acsami.1c17804>.
229. Shang L., Shao J., Ge S. Immunomodulatory Properties: The Accelerant of Hydroxyapatite-Based Materials for Bone Regeneration. *Tissue Eng Part C Methods* 2022; 28(8):377-392. <https://doi.org/10.1089/ten.TEC.2022.0011112>.

Disclaimer/Publisher's Note: The statements, opinions and data contained in all publications are solely those of the individual author(s) and contributor(s) and not of MDPI and/or the editor(s). MDPI and/or the editor(s) disclaim responsibility for any injury to people or property resulting from any ideas, methods, instructions or products referred to in the content.